JOC The Journal of Organic Chemistry

Article

Design of "Click" Fluorescent Labelled 2#-deoxyuridines via C5-{4-(2-Propynyl(methyl)amino)}phenyl acetylene as a Universal Linker: Synthesis, Photophysical Property and Interaction with BSA†

Subhendu Sekhar Bag, and Hiranya Gogoi

J. Org. Chem., **Just Accepted Manuscript** • DOI: 10.1021/acs.joc.7b03097 • Publication Date (Web): 07 Jun 2018

ACS Publications

is published by the American Chemical Society. 1155 Sixteenth Street N.W., Washington, DC 20036

Design of "Click" Fluorescent Labelled 2′-deoxyuridines via C5-{4-(2-Propynyl(methyl)amino)}phenyl acetylene as a Universal Linker: Synthesis, Photophysical Property and Interaction with BSA†

Subhendu Sekhar Bag* and Hiranya Gogoi

†This work is dedicated to Professor Amit Basak (IIT Kharagpur) on his 67th birth day

Bioorganic Chemistry Laboratory, Department of Chemistry, Indian Institute of Technology Guwahati-781039, India. Fax: +91-258-2349; Te.: +91-258-2324; Email: ssbag75@iitg.ernet.in.

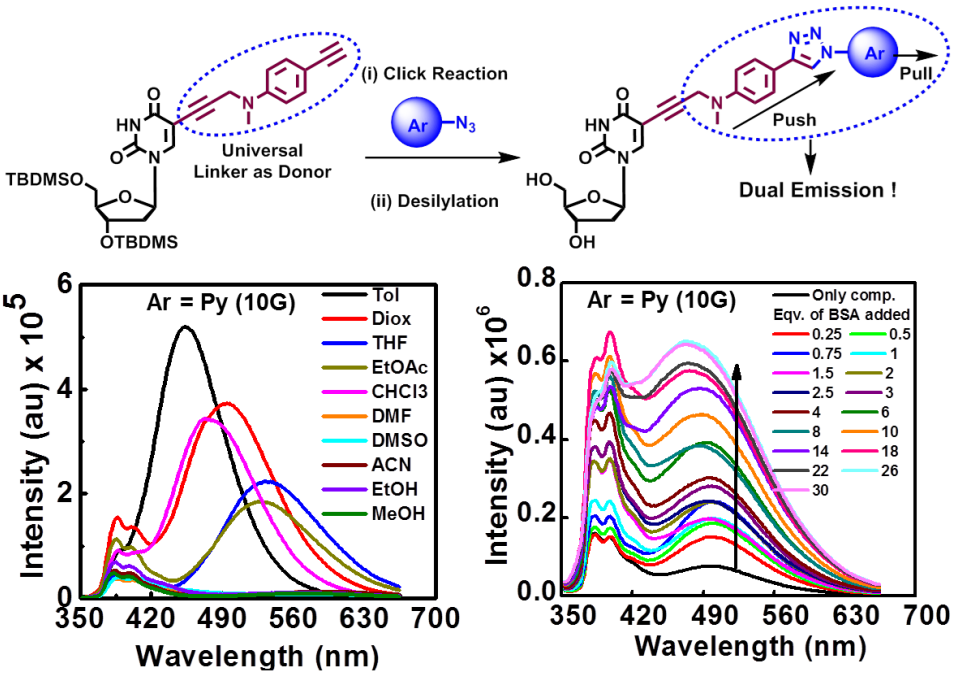

ABSTRACT

Microenvironment-sensitive fluorescent nucleosides present attractive advantages over single emitting dyes for sensing interbiomolecular interactions involving DNA. Herein, we wanted to report the rational design and synthesis of triazolyl push-pull fluorophore labelled

uridines via the intermediacy of C5-{4-(2-propynyl(methyl)amino)}phenyl acetylene as a universal linker. The synthesised nucleosides showedinteresting solvatochromic characteristic and/or intramolecular charge transfer (ICT) feature. Few of them also exhibited dual emitting characteristics evidencing our designing concept. The HOMO-LUMO distribution showed that the emissive states of these nucleosides were characterized with more significant electron redistribution between the C5-{4-(2-propynyl(methyl)amino)}phenyl triazolyl donor moiety and the aromatic chromophores linked to it leading to modulated emission property.The solvent polarity sensitivity of these nucleosides was also tested. The synthesized triazolyl benzonitrile (**10C**), naphthyl (**10E**) and pyrenyl (**10G**), nucleosides were found to exhibit interesting intramolecular charge transfer (ICT) and dual (LE/ICT) emission property. The dual emitting pyrenyl-nucleoside maintained good ratiometric response in the BSA protein microenvironment enabling the switch-on ratiometric sensing of BSA as the only protein biomolecule. Thus, it is expected that the new fluorescent nucleoside analogues would be useful in designing DNA probes for nucleic acids analysis or studying DNA-protein interactions via a drastic change in fluorescence response due to change in micropolarity.

Key words: Fluorophore labelled uredines; triazolyl donor-acceptor; dual emitting nucleosides; microenvironment-sensitive; ratiometric fluorescent nucleosides; sensing BSA.

INTRODUCTION

Polarity sensitive fluorescent molecules are ubiquitous for sensing of biomolecules and studying inter-biomolecular interactions inside a cell.[1] In particular sensing of local microenvironment of DNA is highly important in connection with the detection of DNA mutations causing deleterious effect on cellular survival, high throughput screening and many other biotechnological applications.[2] All these events in DNA rely on novel fluorescent probe-

either as bare or unnatural fluorescent nucleosides or fluorescently labelled natural nucleosides.[3] Though many such probe systems in relation to DNA have been reported but the probes suffer from fluorescence quenching by neighbouring nucleobases or short wavelength emission or poor microenvironment sensitivity.[3a,4] Therefore, designing of novel emissive probes, particularly, fluorescent nucleosides with unique fluorescence properties, extreme sensitivity to change in DNA microenvironment and interactions are highly desirable. Among the three approaches, linking a fluorophore in nucleoside bases is the major approach to generate fluorescent nucleoside useable for DNA sensing.[2-4, 5] As a result of tremendous research efforts, a large number of fluorescently labelled nucleosides and corresponding oligonucleotide probes have been designed and utilised to a variety of applications that include probing DNA hybridization,[6] typing single nucleotide polymorphism (SNP),[7] and monitoring the interbiomolecular interaction,[8] to name a few. However, the majority of the reported environmentally sensitive fluorescent nucleosides exhibited single band emission that sense the differences in micropolarity either by change in emission intensity or wavelength.[9-12] Among these, Saito's ESF nucleosides[13] and fluorene-linked nucleoside by Hocek et al.[14] are highly attractive for monitoring the micropolarity changes within DNA. However, often majority of such probes suffer from several shortcomings such as poor microenvironment sensitivity and low quantum yields.[2-5, 13-14]

Therefore, to overcome these limitations, the concept of two-band emission would be more advantageous over commonly utilised single-band fluorescent probes/nucleosides.[15] Thus, recording a ratio of the intensities at two wavelengths would allow ratiometric sensing which is more advantageous than sensing based on single wavelength emission.[16] Basically, ratiometric sensing results in an intrinsically calibrated emission response.[15] Ratiometric probing of DNA, though reported, but is based on labelling of DNA by two interacting dyes such as FRET pair or excimer/exciplex pair.[6a, 7b, 17] However, labelling with two dyes is

difficult, time consuming as well as highly uneconomical.[15-17] On the contrary, a single fluorophore with dual emission property would be much more beneficial.[18] Highly increased dipole moment and dipole–dipole interactions[1] in the excited state allow such fluorophores to be able to sense the changes in local micropolarity within a biomolecular microenvironment or in cell.[1] Therefore, dual emissive fluorophores are very useful as ratiometric probe because they offer facile and straightforward quantification of a biomolecular event through the ratio of their two bands. However, due to the scarcity of such fluorophores that display dual emissions and the difficulties in their syntheses, the phenomena of dual emission based sensing of biomolecular events are poorly explored, especially, in the field of DNA analysis.[19] With a poor literature reports and the unique ability for sensing the change in the microenvironment of DNA biomolecules, the design of dual emissive modified nucleosides that can control the equilibrium between two excited states at ambient temperature without changing the solvent properties is an unavoidable research area.

As a part of our continuous research efforts in the design of solvofluorochromic molecules/biomolecular building blocks, [20b, 21] we thought that it would be worthwhile to design dual emissive modified nucleosides. Based on our experience, literature reports and wider applicability we considered design of C-5 labeled uridines as model nucleoside probes useable for DNA analysis in future.[3a, 20, 22] However, there is no report wherein C5-position of 2′-deoxyuridine is linked by an electron donor unit as a post-synthetically modifiable functional group which effectively can generate a modulated fluorescence property of a fluorophore if attached at the terminus or the terminal alkyne can be reacted with a fluorophoric azide functionality. Previously, we have shown the "installation/modulation of fluorescence response" of various small fluorescent molecules and an interesting dual emission behaviour from pyrene when attached to *N*,*N*-dimethylanilino triazole donor unit.[23] Inspired by our previous result and motivated by the importance of dual emitting probe for DNA analysis,[19]

we thought that it would be worthwhile to generate a set of fluorescent 2'-deoxyuridine nucleosides which could show interesting intramolecular charge transfer property or dual emission. We further thought that attaching an electron donor phenylacetylene unit as a post-synthetically modifiable functional group at the C5-position of 2'-deoxyuridine would be beneficial to generate a set of fluorescent 2'-deoxyuridines with modulated fluorescence property of a fluorophore via azide-alkyne cycloaddition reaction.[21-22] Furthermore, the same nucleoside if incorporated into DNA can offer the opportunity of generating fluorescent oligonucleotide probes via post synthetic click reaction with modulated fluorescence property.Following the aforementioned design logics herein we report the synthesis of 5-(3-((4-ethynylphenyl)(methyl)amino)propynyl)-2'-deoxyuridineas a possible post-synthetically modifiable nucleoside and its application to generate a set of triazolyl fluorescent 2'-deoxyuridine. Study of photophysical properties of few such fluorescent 2'-deoxy uridines revealed interesting solvatochromic photophysical properties corroborating our design concept. We also tried to support the experimental photophysical properties of three fluorescent uridines by TDDFT calculation.

RESULTS and DISCUSSION

The Design Concept

Our design involves the synthesis of a universal linker, 4-(Propynyl(methyl)amino)phenyl acetylene and its incorporation into C5-position of 2'-deoxyuridine. The universal linker containing 2'-deoxy uridine can then undergo Huisgen 1, 3-dipolar cycloaddition reaction with donor-acceptor chromophore containing fluorogenic azides to afford the target fluorescent uridines. The donor aromatic substituted triazole moiety was thought to allow an intramolecular charge transfer (ICT) process from triazolo-linked moiety to the fluorophoric units leading to solvatochromic fluorescence at a longer wavelength.

Moreover, the fluorophores, such as pyrene, coupled electronically with donor aryltriazoles, could show dual fluorescence property or interesting modulated solvatochromic emission response (Figure 1). Thus, our design would ultimately lead to predetermined photophysical properties of the fluorophores and hence of the nucleoside. The dual fluorescent nucleosides having ratiomatric fluorescence property could be utilised for DNA analysis if incorporated in a DNA for the generation of fluorescent oligonucleotide probes.

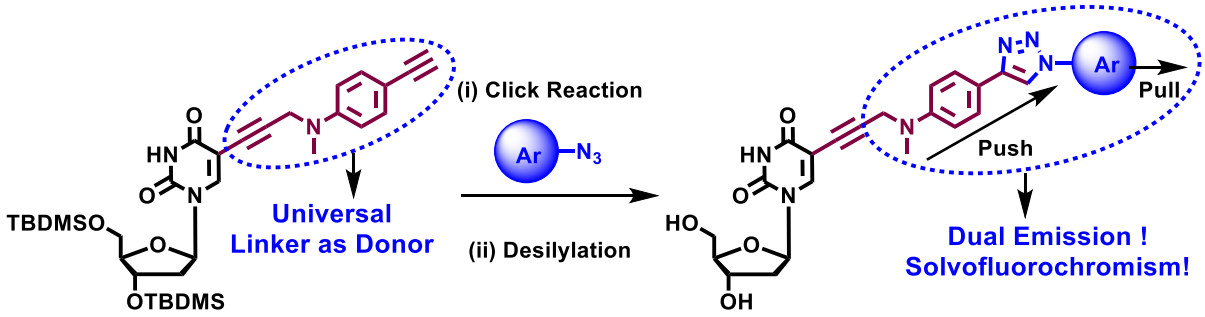

Figure 1. The design concept of dual emitting nucleoside.

Synthesis of the Fluorescently Labelled 2'-deoxy Uridines

To generate a series of target fluorescent uredines, we first synthesised the universal linker containing uridine **8**. Thus, the synthesis was started from N-methyl aniline (**1**) which was converted first to its *p*-iodo derivative **2**. A Sonogashira coupling with trimethylsilylacetylene affording compound **3** underwent propargylation to yield TMS-protected linker unit **4**. The TMS-protected donor acetylene linker was then coupled with bis-TBDMS protected 5-iodo-2'-deoxyuridine through its free propargyl end via a Sonogashira coupling to get compound **7**.[21] The deprotection of TMS group ultimately afforded the bis-protected 2'-deoxy uridine containing donor substituted phenylacetylene as universal linker **8** (Scheme 1). Finally, the universal linker containing uridine was allowed to react with various donor-acceptor substituted fluorogenic aromatic azides (**A-G**, Figure 2) synthesised from the corresponding amines (**H-N;** See SI Figure S1a) under click reaction condition to afford the target fluorescent uredines **9A-G**, in diprotected form, in very good yields (Scheme 1).[23] The final products (See

SI, Figure S1b) were obtained in purity via a silica-gel column chromatography and characterized by NMR and mass spectrometry.

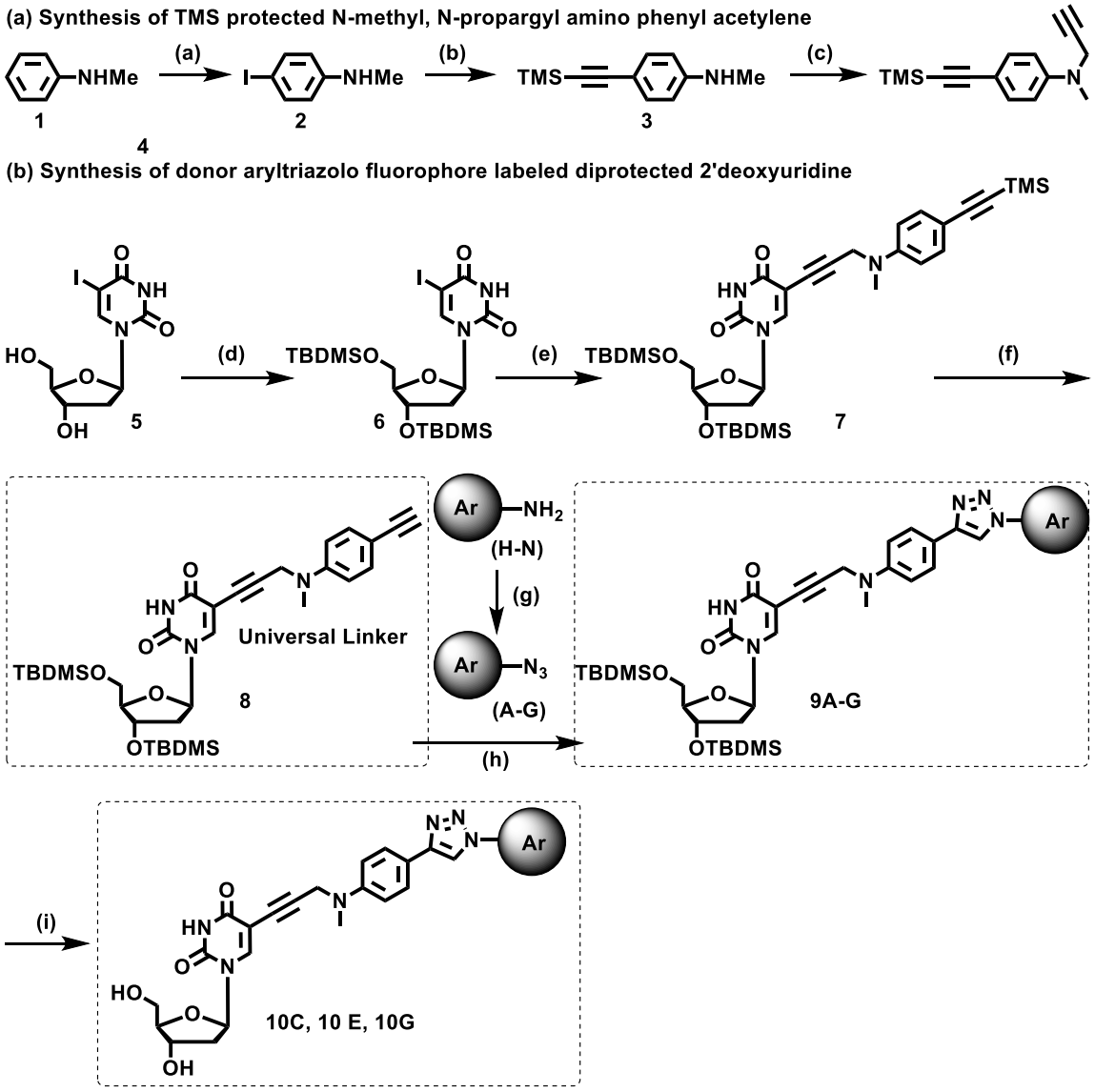

Scheme 1. (a) Synthesis of TMS-protected-{4-(2-Propynyl(methyl)amino)}phenyl acetylene linker (**4**). (b) Synthesis of diprotected C5-(3-((4-ethynylphenyl)(methyl)amino)propynyl)-2'-deoxyuridine as a possible modifiable universal linker nucleoside (**8**) and its various fluorescent analogous 2'-deoxyuridine nucleosides in diprotected (**9A-G)** and in deprotected (**10C, E, G**) form.

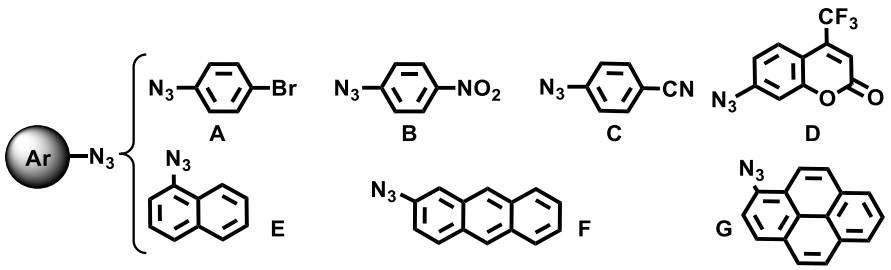

Figure 2. Chemical structures of the synthesised aromatic azides used.

Studies on the Photophysical Properties

The fluorescent nucleosides possessing good solvofluorochromicity are the ideal candidates for utilisation in monitoring change in micropolarity inside and outside a DNA duplex. Therefore, to test whether the synthesised nucleoside would exhibit solvofluorochromic property for future application in generating fluorescent oligonucleotide probe, we next studied their photophysical properties in various organic solvents. We also tried to correlate the solvatochromicity with their donor-acceptor characteristic features. Therefore, after having all the nucleosides in very pure form via silica-gel (60-120 mesh) column chromatography followed by recrystalisation from $CHCl_3$/MeOH solvent mixture, we proceeded to record the UV-visible and fluorescence photophysical properties of few selected synthesised nucleosides.

In general, we observed that the solvent polarity had only a minor influence on the absorption properties of most of the fluorescent nucleosides. However, the fluorescent emission property was modulated enormously upon changing the polarity of the solvents. [23-24] Thus, the analysis of absorption spectra of nitrobenzene containing nucleoside (**9B**) revealed absorptions at 290 and 365 nm in dioxane with very little solvatochromism (by 2-4 nm blue shift). Upon excitation at 365 nm, it showed weak structured emission at around 390 nm with almost similar intensity in all solvents except for EtOH, DMF, $CHCl_3$ wherein enhanced intensity was observed (Fig. 3a-b; SI, Fig S2 and Table S1). A similar absorption pattern with less solvatochromicity was shown by the trifluoromethyl coumarin containing nucleoside (**9D**) with

absorption at 291 and 375 nm. Very weak and broad emission at 445 nm was its characteristic when excited at long wavelength absorption band (Fig. 3c-d; SI, Fig S3 and Table S1).

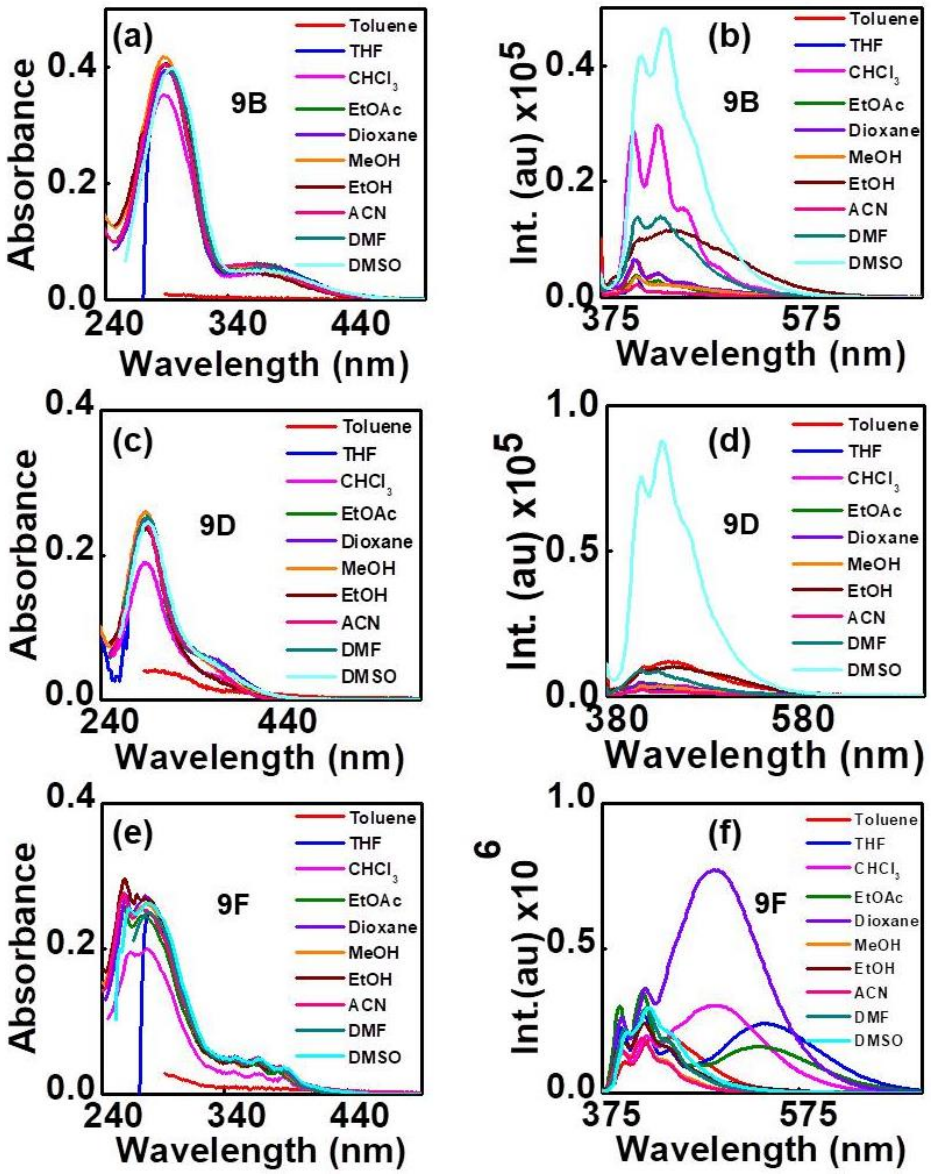

Figure 3. The UV-visible and fluorescence emission spectra of nucleosides **9B** (a-b); **9D** (c-d) and **9F** (e-f) in different solvents (10 μM).

The nucleoside **9F** containing triazolylanthracene exhibited vibronic absorption, characteristic of anthracene at 386, 367, 348 nm, with negligible solvatochromicity. However, it showed interesting emissions when excited at 365 nm. In highly polar and protic solvents it only showed structured emission characteristic of anthracene centered at 415 nm which we

characterized as emission from a locally excited (LE) state. However, in nonpolar solvents such as in dioxane and in moderately polar solvents such as $CHCl_3$, EtOAc and THF the nucleoside exhibited dual emission. It possessed LE emission bands at around 415-420 nm and solvatochromic ICT bands with decreased intensity at 490, 493, 534 and 543 nm in dioxane, $CHCl_3$, EtOAc and THF, respectively (Fig. 3e-f; SI, Fig S4 and Table S1).

Benzonitrile chromophore containing nucleoside **10C** is an interesting fluorescent nucleoside showing highly solvatochromic ICT emission. Thus, the UV-visible spectra showed short wavelength absorption at 288 and long wavelength weak absorption centered at 346 nm in almost all solvents (Figure 4a). Upon excitation at long wavelength absorption band, we observed structureless, broad and strong solvent polarity dependent emission (Figure 4b). It showed a strong emission in dioxane at 471 nm which experienced 80 nm red shift when the polarity of the solvent increased to ACN/DMF (551 nm) with gradual decrease in intensity. In polar protic solvent like methanol, H-bond mediated quenching event resulted in almost no emission.[24a, 25a] Upon titration of a solution of **10C** in dioxane by water a red shift in emission of about 72 nm was observed in 30% water while decreased intensity along with negligible shift in wavelength was the result observed from its absorption spectra in various solvents. Beyond this, addition of further water led to almost full quenching of fluorescence (Figure 4c-d). These features indicated an emission from an ICT state.[23-24, 25b-g] Fluorescence quantum yields are also found to follow the similar trend as solvent polarity was increased (SI, Table S1-4).We measured the fluorescence lifetime for this nucleoside which showed biexponential decay in all solvents following a similar trend as that was observed in steady state emission upon changing the solvent polarity. As for an example, in acetonitrile the average life time and quantum yield were 1.75 ns and 0.04 ns, respectively, while in dioxane the corresponding values were 2.8 ns and 0.34 ns, respectively (Table 1; SI, Fig. S10-S11). This may be because of the fluorescence quenching through non-radiative pathway *via* hydrogen bonding which is

again supported from an increased non-radiative rate constant (K_{nr}) from 2.31 in dioxane to 5.46 in ACN (Table 1).[24a]

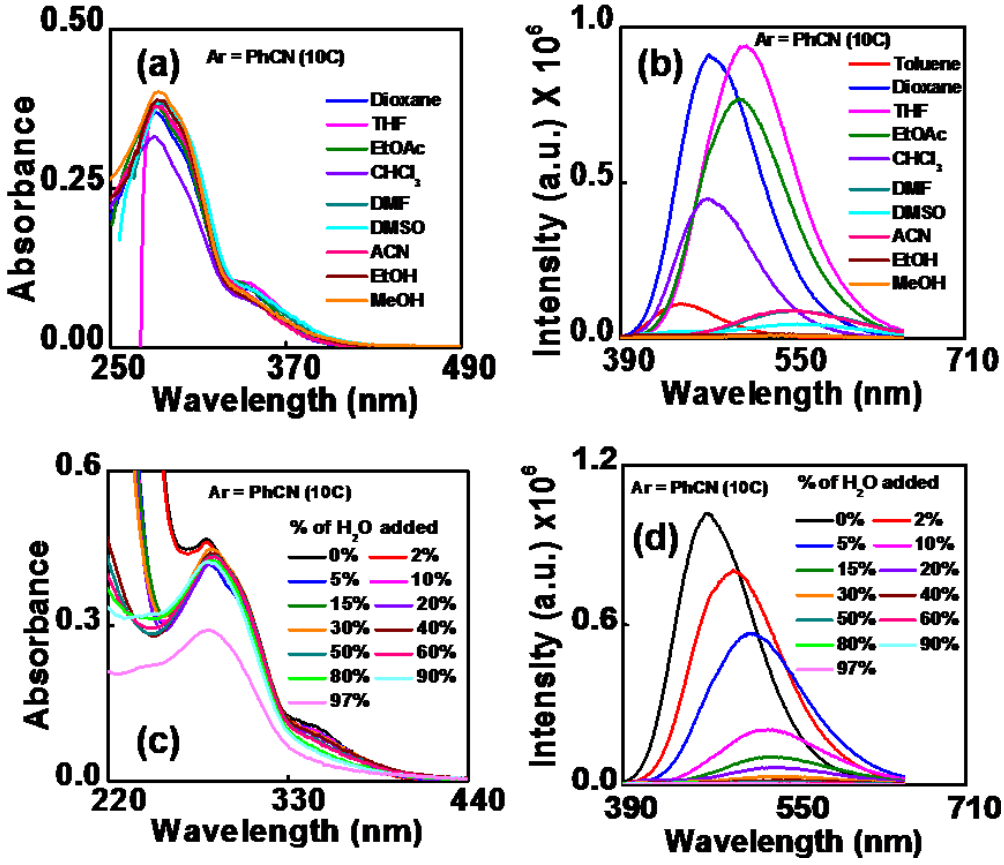

Figure 4. (a) UV-visible, (b) fluorescence emission spectra in various organic solvents for compound **10C**. Dioxane-water titration: (c) UV-visible, (d) fluorescence emission spectra for same. Concentration of the nucleoside **10C** was 10 μM.

Table 1. Summary table of fluorescence lifetimes of the fluorophore **10C**.

Solvents	Dioxane	THF	ACN	$D_{95}W_5$	$D_{85}W_{15}$	$D_{80}W_{20}$	$D_{70}W_{30}$

Properties							
Δf	0.021	0.21	0.305	0.186	0.249	0.262	0.277
λ_{max}^{abs} (nm)	281,338	281,341	282,331	281, 336	282, 334	284, 335	283, 339
λ_{max}^{fl} (nm)	472	507	546	510	530	534	539
Φ_f	0.345	0.291	0.044	0.259	0.055	0.039	0.019
τ_1 [ns]	0.72 (33%)	0.18 (33%)	0.82 (31%)	0.30 (53%)	1.55 (73%)	1.06 (82%)	0.82 (78%)
τ_2 [ns]	3.87 (67%)	4.35 (67%)	2.17 (69%)	4.73 (47%)	4.27 (27%)	4.49 (18%)	3.78 (22%)
k_f [10^8 s^{-1}]	1.22	0.98	0.25	1.08	0.24	0.23	0.13
k_{nr} [10^8 s^{-1}]	2.31	2.38	5.46	3.08	4.13	5.72	6.76
D_pW_q = Dioxane (D) and water (W) solvent mixture; p and q are volume of each solvent.							

The naphthalene containing nucleoside (**10E**) showed structureless absorption at around 288 nm with little solvatochromicity as was revealed both from the spectra in various organic solvents as well as dioxane-water titration (Figure 5a-b). As the polarity increases only a slight increase in intensity was observed. However, strong solvent polarity dependent emission was shown by it that was centered at around 449 nm in dioxane upon excitation at 290 nm. A spectral shift of 80 nm was observed with increase in intensity as we move from dioxane to ACN (529 nm). However, in polar protic solvent, such as MeOH, the intensity and hence the quantum yields were decreased which might be due to H-bonding effect (Figure 5c; Table S1-S3, S5). A dioxane-water titration experiment revealed a red shift of 83 nm (449-532 nm) upto 50% dioxane-water mixture. These results were clearly an indication of an ICT emission. However, addition of 30-60% water revealed another band at 388 nm with increase in intensity. Beyond 70% water the single band at 388 nm was prominent which might be the LE emission (Figure 5d).

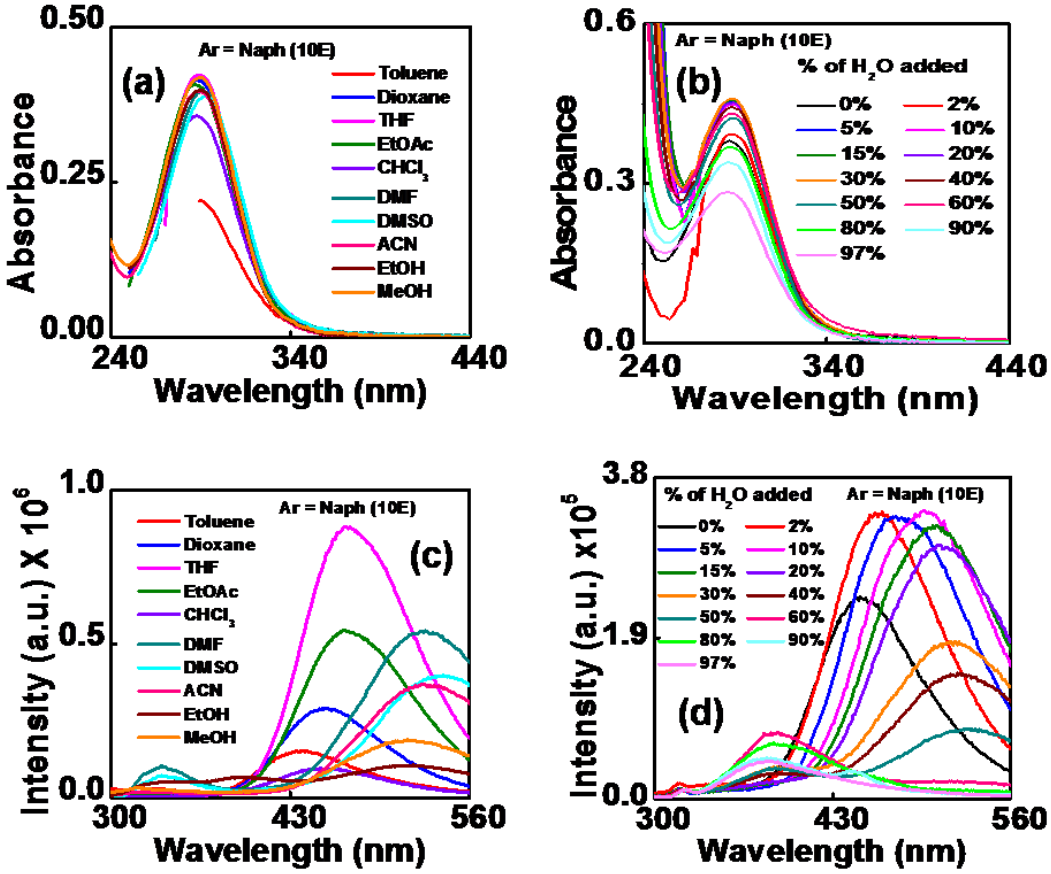

Figure 5. (a-b) UV-visible spectra in various organic solvents and in dioxane-water solvent system, respectively, and (c-d) corresponding fluorescence emission spectra for the nucleoside **10E**. Concentration of the nucleoside **10E** was 10 μM.

Even more interesting photophysics was observed in case of pyrene labeled nucleoside (**10G**) which showed slight blue shifted (by 2-4 nm) solvatochromic absorption of the structured bands at 328 and 344 nm when changing the polarity from dioxane to methanol (Figure 6a). The nucleoside **10G** showed dual emission behavior in low polar solvents like, toluene, dioxane, chloroform, ethylacetate and THF. As the solvent polarity was increased the long-wavelength ICT band at 453 nm in toluene shifted to 537 nm in THF with decreased in intensity. The LE band in these solvents consists of structured pyrene like emission at 385 and 403 nm. However, in highly polar solvent ACN and in polar protic solvent MeOH, EtOH

structured band characteristic of a pyrene emission (only LE emission) had been observed (Figure 6b). A solvatochromicity test in dioxane-water mixture also supported this observation (Figure 6c-d). Thus, the ICT emission at 487 nm was highly dominated over the LE emission in pure dioxane. As the % of H_2O was increased upto 40%, the intensity of ICT band decreased gradually with strong red shift of 89 nm while the intensity of LE emission increased gradually. However, in 50% H_2O in dioxane and beyond we observed pure LE emission (Figure 6d). The fluorescence quantum yield of **10G** also followed the similar trend (SI, Table S1-3, S6-S7).

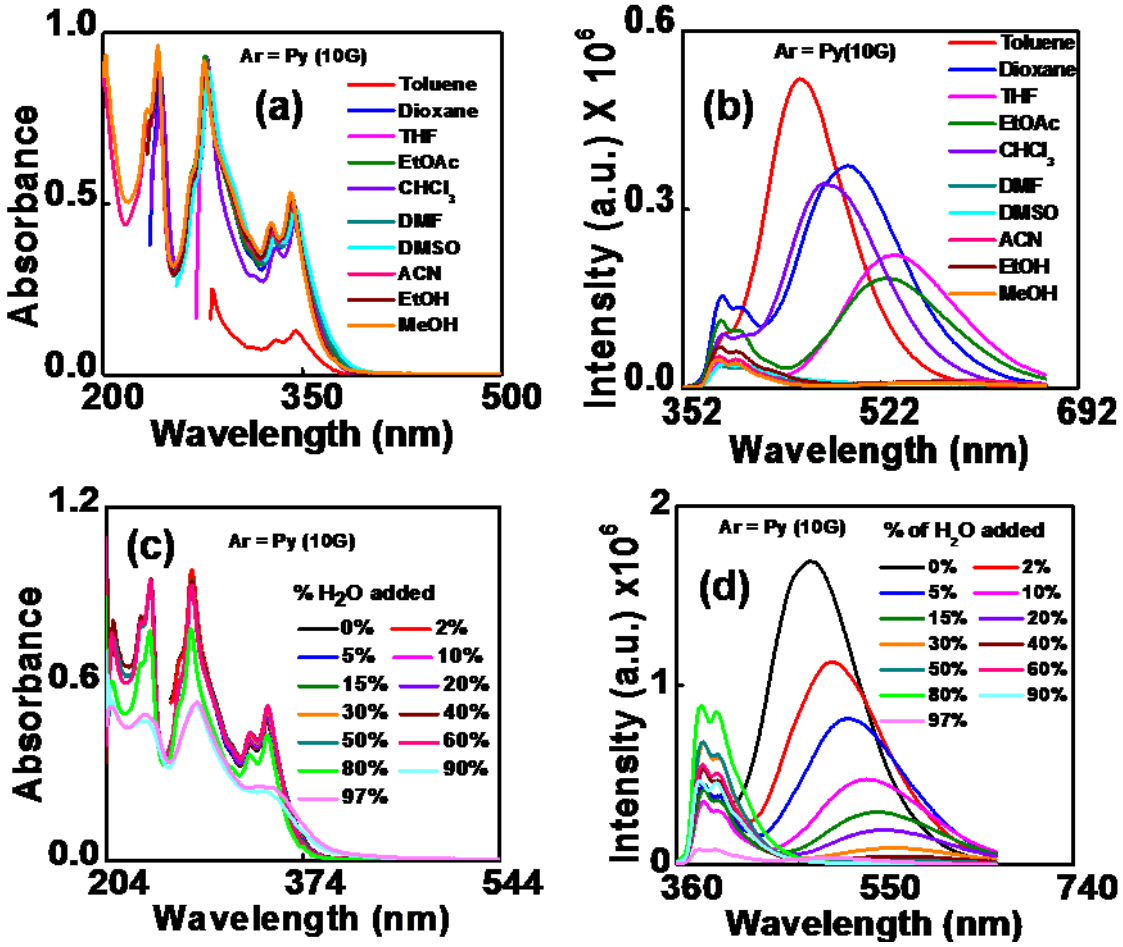

Figure 6. (a) UV-visible, (b) fluorescence emission spectra in various organic solvents for compound **10G**. Dioxane-water titration: (c) UV-visible, (d) fluorescence emission spectra for same. Concentration of the nucleoside **10G** was 10 μM.

To interpret the photophysical properties in a more intuitive manner, the time resolved fluorescence spectra was recorded for pyrenyl nucleoside (**10G**) in different solvents which also supported observations of steady state fluorescence. Thus, we collected the lifetime data by monitoring both at LE and ICT bands with an excitation light of 337 nm which displayed biexponential decays (Table 2; SI, Table S6-7). The relative contribution of the longer lifetime component (τ_2 = 10.88 ns) in dioxane was found to decrease from 49% to 39% as the solvent polarity was increased (in THF, τ_1 = 7.13 ns) while the same was increased from 51% (τ_1 = 0.99 ns) to 61% (τ_1 = 0.66 ns) for the case of shorter life time component when the decay was monitored at LE emission (400 nm). In methanol, the component contributing 49% has decay time τ_2 = 7.64 ns while the other component having decay time τ_1 = 0.59 ns contribute 51% suggesting only a weak emission from LE state and the chromophoric unit followed a non-radiative pathway producing no ICT emission in methanol (Table 2). Furthermore, the value of τ_1 and τ_2 remain consistent while the relative contributions of the two lifetimes vary according to the observed wavelength in dioxane and THF. Thus, the contribution from longer lifetime component τ_2 increased from 49% to 57% as the monitoring wavelength was changed from 400 nm to 495 nm in dioxane solvent. Similar behavior was observed in THF solvent. The decreased intensity of ICT band was also reflected by the decreased lifetime from τ_1 = 0.13 (in dioxane) to τ_1 = 0.06 ns in THF (Table 2; SI, Fig. S12-13). Furthermore, the value of τ_1 and τ_2 remain consistent while the relative contributions of the two lifetimes vary according to the observed wavelength in dioxane-water solvent mixture (Table 2).

Table2. Summary table of fluorescence property of nucleoside **10G** in various solvents.

Solvents / Properties		Dioxane	THF	ACN	$D_{95}W_5$	$D_{85}W_{15}$	$D_{70}W_{30}$	$D_{50}W_{50}$
Δf		0.021	0.21	0.305	0.186	0.249	0.277	0.294
λ_{max}^{abs} (nm)		328, 343	343	327, 341	328 , 343	328 , 343	328 , 343	328, 343
λ_{max}^{fl} (nm)		387, 400, 494	386, 403, 533	384, 400, 590	386, 401, 526	386, 401, 550	386, 400, 570	385, 399, 580
LE	Φ_f	0.007	0.002	0.003	0.024	0.022	0.038	0.038
	τ_1[ns]	0.9(51%)	0.6(61%)	1.0 (42%)	1.5(32%)	1.4(29%)	1.8(26%)	2.2(21%)
	τ_2[ns]	10.8(49%)	7.1(39%)	11.7(58%)	23.4(68%)	26.8(71%)	28.4(74%)	29.3(79%)
	k_f	0.012	0.006	0.004	0.015	0.011	0.017	0.016
	k_{nr}	1.68	3.13	1.37	0.60	0.50	0.44	0.41
ICT	Φ_f	0.054	0.035	0.002	0.027	0.01	0.003	0.0005
	τ_1[ns]	0.13(43%)	0.06(49%)	0.1(40%)	0.3(49%)	0.2(56%)	0.1(56%)	0.3(92%)
	τ_2[ns]	1.3 (57%)	1.9 (51%)	1.4 (60%)	3.4(51%)	1.3(44%)	1.3(44%)	1.31(8%)
	k_f	0.71	0.35	0.021	0.14	0.15	0.05	0.013
	k_{nr}	12.44	9.55	10.73	5.23	15	15.82	25.63

k_f and k_{nr} in 10^8 s^{-1}; D_pW_q = Dioxane (D) and water (W) solvent mixture; p and q are volume of each solvent.

To get an insight into the different solvatochromic behaviours of benzonitrile (**10C**), naphthyl (**10E**) and pyrenyl (**10G**) nucleoside, the spectral dependency on solvent polarity was studied on the basis of Lipert-Mataga model.[26a] The polarity parameter of various solvents were calculated from the following equation 1.[26]

$$\Delta f = \frac{\varepsilon - 1}{2\varepsilon + 1} - \frac{n^2 - 1}{2n^2 + 1} \qquad (1)$$

We tried to correlate the absorption and fluorescence maxima ($\tilde{\nu}_{max}^{abs}$ and $\tilde{\nu}_{max}^{fl}$, respectively, in cm^{-1}) with the solvent polarity parameter Δf for the nucleoside **10C**, **10E** and **10G** (Figure 7a-c). Thus, from the plots it was clear that for all the cases, the $\tilde{\nu}_{abs}$ values apparently correlate linearly with Δf values. This indicated that the ground state of these fluorophoric nucleoside were moderately polar in nature. However, the $\tilde{\nu}_{fl}$ values for all the nucleosides showed a very good linear correlation with Δf for the whole range of the solvent polarity tested indicating that the nature of the fluorescent states remained essentially unchanged in all the solvents for all cases. However, due to the modulation by the solvents, the spectral feature changes significantly. The highly polar nature of the fluorescence states of these nucleosides were

evident from the high slopes of the $\tilde{\nu}_{fl}$ vs Δf plots indicating their possible intramolecular charge transfer (ICT) character.[23-25, 27]

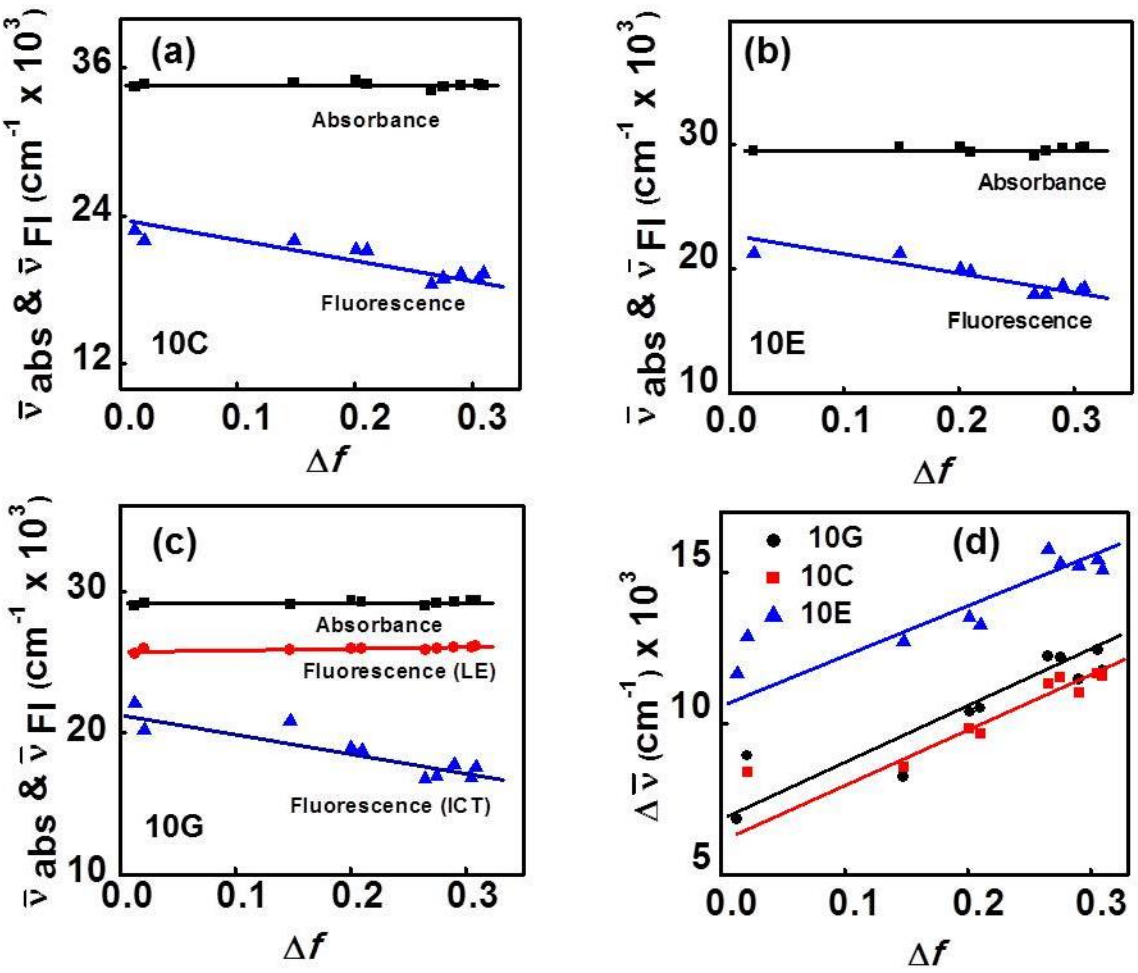

Figure 7. Plots of $\tilde{\nu}_{fl}$ and $\tilde{\nu}_{abs}$ values against Δf for fluorescently labelled nucleoside **10C** (a), **10E** (b) and **10G** (c) ($\tilde{\nu}_{fl(ICT)}$ and $\tilde{\nu}_{abs}$ values) in different solvents. (d) Plot of $\Delta\tilde{\nu}$ values against Δf in different solvents for **10C**, **10E** and **10G**.

Next, the Stokes' shift ($\Delta\tilde{\nu}$) was plotted against Δf following the Lippert and Mataga equation 2[26] where μ_e and μ_g are the excited (fluorescent) state and the ground state dipole moments of the fluorophore, h is Planck's constant, c is the velocity of light and r is the Onsager radius of the dipole-solvent interaction sphere.

$$\Delta\tilde{\nu} = \Delta\tilde{\nu}_0 + \frac{2(\mu_e - \mu_g)^2}{hcr^2}\Delta f \qquad (2)$$

The linear plot with large slopes suggested a good correlation between $\Delta\tilde{\nu}$ values for all the three nucleosides, **10C**, **10E** and **10G** (long wavelength emissive band) in different solvents (Figure 7d) indicating the fluorescence states are highly polar in nature.

Theoretical Calculation

We next carried out theoretical calculation to support the observed polarity-dependent emission and the ICT feature using Gaussian 09 program package.[28] The possible transitions obtained from a TDDFT calculation, were, thus, analysed (Figure 8; SI, section 5). From the HOMO-LUMO overlap and transition oscillator strength, it is clear that the $S_0 \rightarrow S_1$ electronic transitions are fully allowed for all the three representative nucleosides indicating the reverse transition, *i.e.*, $S_0 \leftarrow S_1$, as fully allowed. Redistribution of electronic charge density was reflected from an overlap in HOMO-LUMO supporting the solvatochromicity and intramolecular charge transfer emissions (Figure 8).[23, 29] As for example, except for coumarin (**9D**), the TDDFT calculations suggested the $S_0 \rightarrow S_1$ transitions with high configuration interaction (CI) values as the dominant orbital transitions in the low-lying singlet excited states of the studied nucleosides. Interestingly, the universal linker unit with the triazole at C5-position of 2'-deoxyuridine comprised the HOMO, while the aromatic fluorophoric unit irrespective of their substituents formed the LUMO in all the studied nucleosides supporting our designing concept. Except for the case of coumarin (**9D**), the triazole unit overlapped with the LUMO of the chromophore indicating a good electronic redistribution and ICT character (SI, section 5).

Thus, the calculated excitation energy for the transition $S_0 \rightarrow S_1$ for pyrene (**10G**) and benzonitrile (**9C**) containing fluorescent nucleosides were found to be 436 nm (2.84 eV, f = 0.1299; CI = 0.704); 407 nm (3.05ev, f = 0.217, CI = 0.705) (in vacuum), respectively. These values co-related with the experimental results of 343 nm (THF) and 346 nm (THF)

respectively. Other two prominent transitions are at 414.8 nm (2.98 eV; f = 0.0006; CI = 0.703) and 348.8 nm (3.56 eV; f = 0.508; CI = 0.641) for pyrenyl nucleoside and at 376.4 nm (3.29 eV; f = 0.0010; CI = 0.705) and 315 nm (3.93 eV; f = 0.0551; CI = 0.702) for benzonitrile nucleoside (Figure 8a-b). For the case of naphthalene (**10E**) and coumarin (**9D**) labelled nucleosides, along with weak $S_0 \rightarrow S_1$ transition (f = 0.0046/0.0008), the prominent transitions are observed from $S_0 \rightarrow S_2$ and $S_0 \rightarrow S_3$, respectively (SI, section 5) indicating the emissive states of these nucleosides as LE state.

From the strong HOMO-LUMO mixing it is clear that the emissive state of bezonitrile (**10C**) is characterized with more significant electron redistribution, *i.e.*, ICT feature**.** The calculations rationalized the explanation of ICT origin of the solvent polarity dependency of the nucleosides' emission (Figure 8a). The pyrene nucleoside (**10G**) showed dual emission. The long wavelength band is highly sensitive to polarity of the solvent i.e., ICT origin. Thus the dual emission comes from both LE and CT states. The transition from HOMO-1 to LUMO is closer to the experimental value with higher *f* value (*f* = 0.508) indicating that the S_2 state is populated well (Figure 8b; SI, Section 5.3).

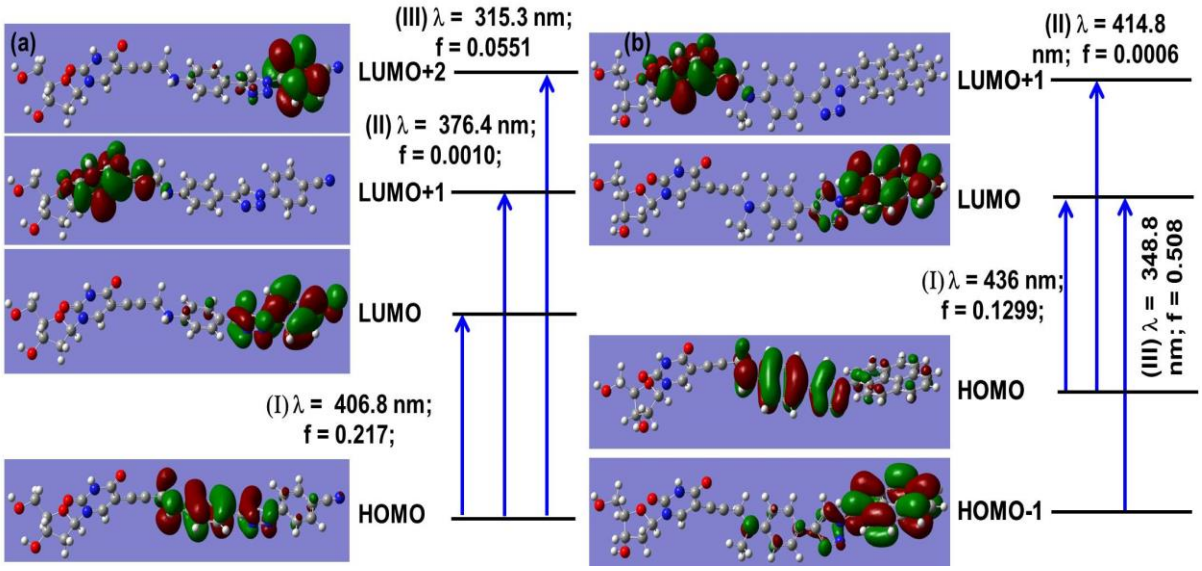

Figure 8. The possible transitions from TD-DFT calculation for the representative nucleosides containing (a) benzonitrile (**10C**) and (b) pyrene (**10G**).

Study of Interaction with BSA

Finally, the dual emitting nucleosides, in particular the pyrenyl nucleoside, **10G**, is both fundamentally and conceptually new and novel which could serve as sensitive probe for studying nucleoside-protein/nucleoside-DNA interaction and in other wider applications.[30] Understanding the nature of drug-protein interactions or small molecule-protein interaction is of paramount importance for the development of new chemotherapeutics. Since last 50 years, the nucleosides analogues have become the corners stone for clinical use for the treatment of cancer or viral infections. However, only about 40 nucleoside analogues have been approved for clinical use till the date and few are in clinical trials.[31] Despite their broad range of biological activity, many nucleosides could not find applications as drugs mainly due to poor cell membrane penetrability.[31-32] Furthermore, the nucleoside metabolism is vital to cellular survival. About half of all enzymes are nucleoside-dependent. Therefore, study of nucleoside-protein interaction and understanding the structure–function relationships of nucleoside-binding proteins are highly important to get functional insights for many proteins.[31-32] Therefore, immense clinical importance of nucleosides and their analogues put in force to accumulate knowledge how they are being recognized and transported into the cell. Understanding such events could not only provide knowledge about nucleoside-related biological processes but also help designing of new nucleoside derivatives as possible drugs.[33] Furthermore,the biological roles of nucleosides are dependent on specific interaction with cellular proteins. As for an example, nucleotide-protein interactions are considered critical in the action of some purine nucleoside analogs or isoniazid drugs that have recently been for the treatment of Mycobacterium tuberculosis (Mtb) infections.[34]

Selective binding of small molecules/nucleosides have great impact on the functions of many proteins, especially with plasma proteins. Therefore, study of specific interaction with nucleoside/ nucleotide and plasma proteins is highly important. In this view, we, therefore,

thought that the dual emission from the new nucleoside **10G** might offer some interesting insight into the interaction with a biomolecule such as a model protein bovine serum albumin (BSA). With 76% sequence identity to human serum albumin (HSA), BSA is widely used as a model protein in investigating protein-drug interaction in detail.[35] Moreover, BSA is experimentally well accessible. Similar to HAS, BSA contain three linearly arranged domains (I–III). It has two major drug binding sites situated in the subdomains IIA (site I) and IIIA (site II).[36] The two tryptophan (Trp) residues, Trp134 and Trp 212, are located in the outer hydrophilic environment and in the hydrophobic binding pocket of site I of BSA which is widely used to study drug-BSA interaction fluorimetrically.[37] Thus, we finally decided to study the interaction of **10G** with model protein BSA using UV-visible and fluorescence spectroscopy. Our main aim was to test whether the pyrenyl fluorescent nucleoside **10G** could interact with any biomolecule, such as a protein biomolecule. Moreover, we wanted to know that in protein's microenvironment the nucleoside probe whether could retain its dual emission property. Therefore, at this stage, we did not consider the probes for studying interaction with other proteins to test their protein binding specificity. This extended study along with the study with DNA biomolecule is under consideration of our laboratory.

The UV-visible spectra in phosphate buffer revealed that the probe nucleoside **10G** exhibited very weak, broad and structureless short and long wavelength absorptions at around 283 and 351 nm. The characteristic pyrenyl absorption was not present in contrary to that in the organic solvent. Upon gradual addition of BSA to a solution of the probe, the absorption bands experienced strong hyperchromicity and hypsochromic shift of 5-7 nm along with appearance of characteristic pyrenyl bands at around 345 and 329 nm. This indicated a strong binding interaction of the probe in the hydrophobic region of BSA (Figure 9a; SI, Section 6). The Job's plots suggested a 1:1 probe: BSA binding events (Figure 9b). The association

constant was also evaluated from a Benesi-Hildebrand plot showing value of 1.0 x 10^4 M^{-1} and binding free energy -5.5 kcal/$mole^{-1}$ (Figure 9c; SI, Section 6).[30, 32]

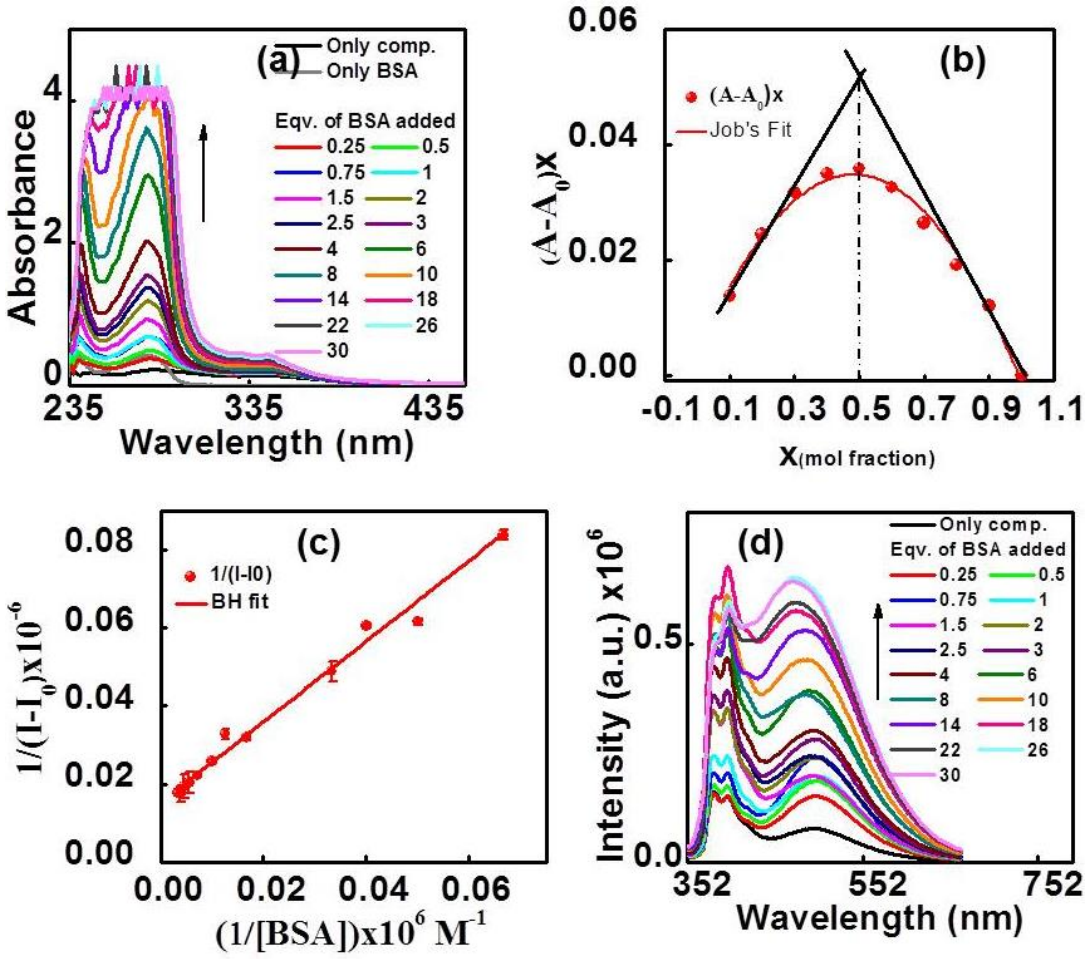

Figure 9. (a) UV-visible spectra of **10G** in absence or in presence of BSA. (b) Absorption Job's plot of probe, **10G** in presence of BSA protein indicates a 1:1 stoichiometry of the probe to BSA in the complex. (c) Benesi-Hildebrand plot. (d) Fluorescence emission titration spectra of **10G** in absence or in presence of BSA (λ_{ex} = 342 nm).The probe concentration [**10G**] =10μM.

Next, a fluorescence titration experiment was carried out to investigate the BSA sensing ability. In buffer, the probe showed dual emission, LE (at 381, 398 and 427) band characteristic of pyrene and ICT band at 501 nm. Interestingly, the nucleoside **10G** retained its dual emitting

property in all the concentration of BSA. It showed a regularly increased in both the LE and ICT bands when excited at 343 nm upon gradual addition of an increasing amount of BSA (Figure 9d). The quantum yield variations also supported the same. Thus, the quantum yields of only probe, 1:1 Probe: BSA, 1:22 and 1:30 probe (**10G**): BSA in 2% DMF in buffer were found to be 0.0025 (LE), 0.003 (ICT); 0.006 (LE), 0.006 (ICT); and 0.009 (LE), 0.014 (ICT), 0.007(LE), 0.015 (ICT); respectively (SI, Table S8). While position and shape of the LE band remained unaltered, peak broadenings and blue shits were the major results of ICT bands with increasing concentration of BSA similar to what was observed in organic solvents or in dioxane-water titration experiments of the probe (SI, Figure S7). All these observations clearly suggested the accommodation of the fluorophoric pyrenyl moiety of the probe inside the hydrophobic pocket of BSA. Therefore, even in the BSA microenvironment, the probe **10G** behaved as a system of dual emitting switch-on fluorescent probe.

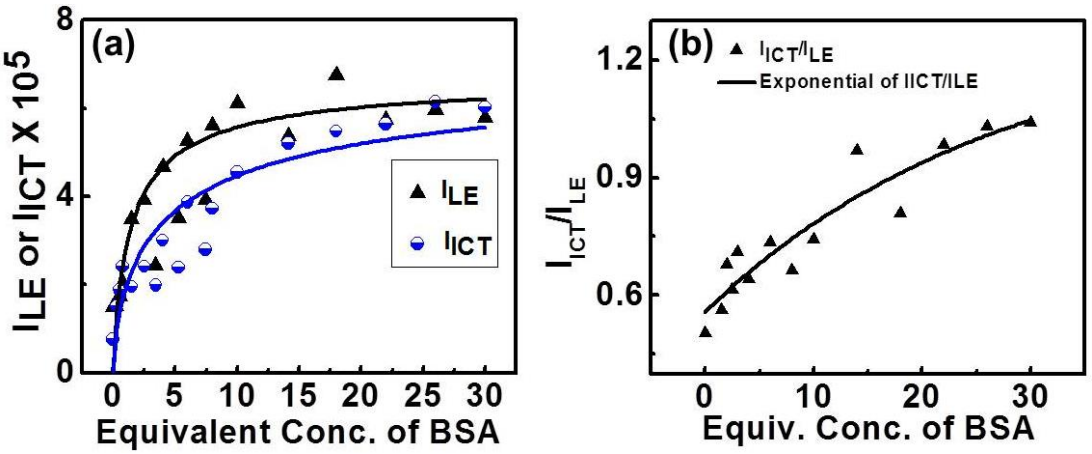

Figure 10. (a) Plot of intensity of LE or ICT and of (b) LE/ICT vs. equivalent conc. of BSA added. The probe concentration [**10G**] =10μM.

The LE, ICT fluorescence intensity and the I_{LE}/I_{ICT} ratio (I_{398}/I_{500}) were plotted against the equivalent concentration of BSA added to clearly demonstrate the fluorescence behaviour of the ratiometric fluorescent pyrenyl nucleoside probe. Thus, from the plot in figure 10a it is

clear that the intensity of both the LE and ICT bands increased upto 14 equivalent of BSA with respect to 10 μM probe concentration. Further addition of BSA does not induce notable change in both LE and ICT bands. The same plot for ratio LE/ICT vs. equivalent concentration of BSA added shows that the LE/ICT values decreased or ICT/LE increases exponentially indicating that the probe nucleoside **10G** functions as a good ratiometric BSA sensor (Figure 10b).[38] Ratiomatric fluorescence sensing offers increased signal-to-noise ratio leading to more reliable quantification compared to that by using a probe of emission at a wavelength.[39] Furthermore, ratiometric fluorescence is more reliable compared to absolute fluorescence intensity in demonstrating sensing events because the ratios do not suffer from simultaneous drifts or fluctuations of individual signals.[40] Therefore, the probe nucleoside **10G** could find wide applications in ratiometric sensing in chemistry, biology and in materials sciences.[38-40]

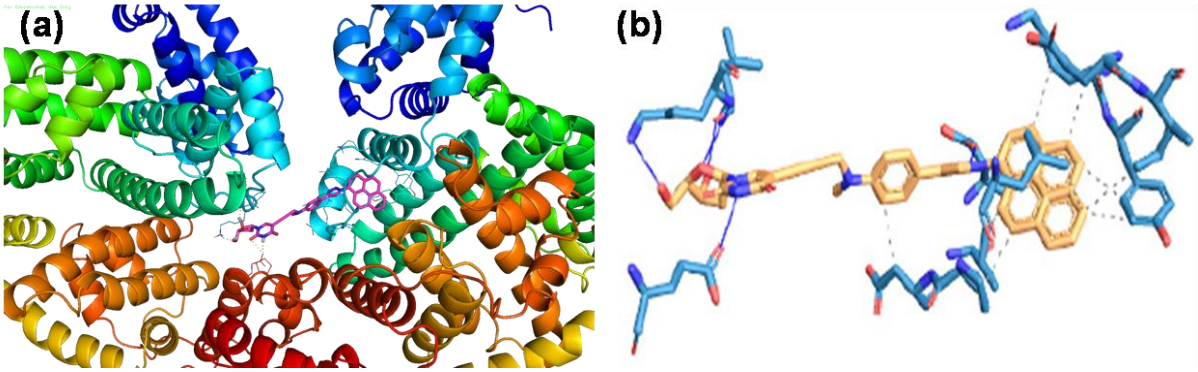

Figure 11. (a) Docking pose and (b) various interactions of the nucleoside **10G** inside the hydrophobic pocket of BSA.

Finally, we carried out molecular docking calculation to get insight into the binding site of the probe nucleoside using Autodock 4.2.[41] From the docking study, it is clear that the dual emitting pyrenyl nucleoside **10G** binds to both the chains of BSA. As revealed from the docking pose in figure 11a, the Leu115, Pro117, Asp118, Leu122, Lys136, Glu 140, Ile141

and Tyr137 residues of chain B was involved in hydrophobic interactions mostly with the chromophoric phenyl triazolyl pyrenyl unit.[30, 42] The π-stacking between pyrenyl unit and the closely spaced Tyr made the association strong. On the other hand, the uridine ring and the sugar-OH functionalities are involved in strong H-bonding interactions with Leu112, Lys114 and Glu519 of chain A and Glu125 of chain B of BSA leading to increased association (Figure 11b). The overall free energy change associated with the interaction of the probe nucleoside with BSA obtained from molecular docking was found to be -9.2 kcal/mol. The α-helicity of the BSA upon binding to the probe remained unperturbed as was evident from a CD spectral titration. The slight increase in intensity and % α-helicity of BSA was possibly because of conformational adjustment of BSA upon association with the probe nucleoside (SI, Section 6.5).

SUMMARY and CONCLUSION

Therefore, all the experimental and theoretical results clearly showed that the fluorogenic aromatic azides having no substituent or electron withdrawing substituent, such as –CN, upon reaction with the universal donor phenylacetylene linker of the 2'-deoxyuridine under "click" reaction condition would able to generate interesting fluorescent nucleoside. The main importance of our work is that we utilized a simple donor phenylacelene as linker to generate solvatochromic fluorescent nucleoside via click reaction with readily available fluorogenic aryl azides. The linker labelled nucleoside would be useful in generating oligonucleotide which can be made fluorescent post-synthetically and can then be utilised as probe for DNA analysis. Furthermore, the fluorophoric moieties in these nucleosides showed a direct correlation between the fluorescence intensities and the solvent polarity. All these results along with the fluorescence band-shape and quantum yields revealed a correlation between the D-A structure and the emissive states. That the emissions from the nucleoside **10C**, **10E** and **10G** were

originating from ICT states, indicated by their strong fluorescence emission with broad band-shapes, high quantum yield, high solvofluorochromicity. In addition to that, the nucleoside **10G** exhibited solvent polarity independent LE emission originated from a non-polar $^1\pi$–π^* state. Therefore, the dual emission as was observed for nucleoside **10G**indicated the presence of a mixed LE and CT state wherein the switching between these two states depends on the structure and the solvent polarity.

The strong polarity sensitive ICT emission from these nucleosides can be utilized in monitoring the change in micropolarity inside and outside a DNA duplex. Thus, these nucleosides would be useful in generating fluorescent oligonucleotide probes for DNA analysis. Furthermore, the sensing index derived from the intensity ratio between ICT and LE emission could be employed for the same. The dual emitting fluorescent pyrene containing nucleoside would impact greatly in nucleoside research as rare examples of such nucleosides exist in literature. Further, the donor phenylacetylene linker reported here is interesting and would find wide applications in generating fluorescent nucleosides or post synthetically derived fluorescent oligonucleotide probes. Our current research activity focuses in this direction. Finally, the preliminary study suggested that the dual emitting nucleoside was efficient to interact with BSA via a switch on fluorescence and was able to retain its photophysical property in the biomolecular microenvironment. As the ratiometric fluorescence sensing is highly advantageous compared to a single wavelength emission, the ratiometric fluorescent nucleoside probe **10G** would find wide future application in chemistry, biology and in material sciences.

EXPERIMENTAL SECTION

Materials and Methods

All reactions were carried out under inert atmosphere using flame-dried glassware. Combined organic layers were dried over anhydrous sodium sulphate. After work up solvents were removed in a rotary evaporator under reduced pressure. For column chromatography Silica gel (60- 120 mesh) was used. Reactions were monitored by TLC on silica gel 60 F254 (0.25). ^{1}H NMR spectra were recorded either at 400MHz or at 600 MHz and ^{13}C NMR spectra were recorded either at 100 MHz or at 125 MHz (mentioned accordingly). Coupling constants (*J* value) were reported in hertz (Hz). The chemical shifts were shown in ppm downfield form tetramethylsilane, using residual chloroform (δ = 7.26 in ^{1}H NMR, δ = 77.23 in ^{13}C NMR) or DMSO (δ = 2.5 in ^{1}H NMR, δ = 39.5 in ^{13}C NMR) as an internal standard. All the NMR-FID has processed in MestReNova v6.0.2 software. High-resolution mass spectra (HRMS) were recorded on a Mass spectrometer in positive mode using electrospray ionization-time of flight (ESI-TOF) reflection experiments. IR spectra were recorded on KBr plate in a FT-IR spectrophotometer and reported in frequency of absorption (cm^{-1}).

Characterisation

Synthesis of 4-iodo-N-methylaniline (2): This compound was synthesised following a modified literature procedure. [43a] *N*-methylaniline (**1**, 3.95 g, 13.84 mmol) was taken in a round bottom (R.B.) flask and was dissolved in 20 ml of pyridine: dioxane (1:1). The resulting reaction mixture was cooled to 0 ^{o}C in an ice bath and half of the total 5.6 g (22.14 mmol) of I_2 was added to it. While maintaining the ice cooled condition, remaining half amount of I_2 was added after 2 hours. After stirring for about 3 h, ice bath was removed and the reaction mixture was stirred at room temperature for another 22 h. After completion of reaction, monitored by TLC, the reaction mixture was partitioned between ethyl acetate and water. Collected organic layer was washed with saturated sodium thiosulfate solution, water and brine solution. After evaporation, the crude product was purified by column chromatography (Si-gel, Hex: EtOAc

= 30:1) to obtain the 4-iodo-N-methylaniline**2** as dark yellow liquid. Yield 92 % (7.97 g).^{1}H NMR ($CDCl_3$, 400 MHz): δ 7.4 (d, *J* = 8.4 Hz, 2H), 6.36 (d, *J* = 8.4 Hz, 2H), 3.71 (s, 1H), 2.767 (s, 3H); ^{13}C NMR ($CDCl_3$, 100MHz): δ 148.9, 137.8, 114.7, 77.7, 30.6.

Synthesis of N-methyl-4-((trimethylsilyl)ethynyl)aniline (3): This compound was synthesised following a modified literature procedure. 5 g (21.45 mmol) of 4-iodo-N-methylaniline (**2**) was taken in a dry R.B. and dissolved in 20 ml of dry benzene. To the above solution 10 ml of dry n-butylamine was added and the resulting mixture was degassed for 10 minutes by bubbling N_2 through it. $PdCl_2(PPh_3)_2$ (0.45 g, 0.03 mmol) followed by CuI (0.04 g, 0.01 mmol), were added to the reaction mixture while continuing the degassing. Finally, trimethylsilylacetylene (3.16 g, 32.17 mmol) was added to the reaction mixture and it was refluxed (70-80 °C) under N_2 atmosphere for 7 hours. After completion of reaction, the reaction mixture was partitioned between ethyl acetate and water. Collected organic layer was washed with aqueous ammonium chloride solution, water, brine solution and dried over anhydrous Na_2SO_4. After evaporation, the crude product was purified by column chromatography (Si-gel, Hex: EtOAc = 30:1) to obtain product **3** as reddish brown liquid. Yield: 83% (3.62 g). IR (KBr)ν̃ 3421, 2147, 1609, 1521cm^{-1}; ^{1}H NMR ($CDCl_3$, 400 MHz): δ 7.06 (d, *J* = 8.8 Hz, 2H), 6.23 (d, *J* = 8.8 Hz, 2H), 3.64 (s, 1H), 2.56 (s, 3H), 0.00 (s, 9H); ^{13}C NMR ($CDCl_3$, 100 MHz):δ 149.5, 133.4, 111.8, 106.6 , 91.1, 30. 4, 0.7. **+ESI-HRMS** calculated for $C_{12}H_{18}NSi$ **[M+H]**$^{+}$204.1203, found 204.1198.

Synthesis of N-methyl-N-(prop-2-yn-1-yl)-4-((trimethylsilyl)ethynyl)aniline (4): This compound was synthesised following a modified literature procedure.[43b] 2.5 g (12.29 mmol)of *N*-methyl-4-((trimethylsilyl)ethynyl)aniline (**3**) was taken in a R.B. and dissolved in 8 ml of dry DMF. Anhydrous K_2CO_3 (2.55 g, 18.44 mmol) was added to the mixture followed by propargylbromide (2.19 g, 18.44 mmol). The resulting reaction mixture was stirred at 50 ^{o}C for 15 hours under N_2 atmosphere. After completion of reaction, the reaction mixture was

partitioned between ethyl acetate and water. Collected organic layer was washed with water, brine solution and dried over anhydrous Na_2SO_4. After evaporation, the product was purified by column chromatography (Si-gel, Hex: EtOAc = 30:1) and obtained as brown semi solid. Yield: 79 %(2.36g). IR (KBr)ν̃3279, 2147, 1883, 1605, 1517cm^{-1};^{1}H NMR ($CDCl_3$, 400 MHz): δ 7.36 (d, *J* = 8.4 Hz, 2H), 6.71 (d, *J* = 8.4 Hz, 2H), 4.05 (d, *J* = 1.6 Hz, 2H), 2.98 (s, 3H), 2.17 (s, 2H), 0.2 (s, 9H); ^{13}C NMR ($CDCl_3$, 100 MHz):δ 148.9, 133.3, 113.4, 106.2, 91.9, 79.0, 7 2.3, 42.2, 38.5, 0.3. **+ESI-HRMS** calculated for $C_{15}H_{20}NSi$ **[M+H]**$^+$242.1360, found 242.1356.

Synthesis of3',5'-di-O-tert-butyldimethylsilyl-5-iodo-2'-deoxyuridine (6):This compound was synthesised following a modified literature procedure. [44a] 4 g (11.23 mmol) of 5-iodo-2'-deoxyuridine (**5**) was taken in a dry R.B. and dissolved in dry DMF. The reaction mixture was vacuumed and filled with N_2. Imidazole (3.85 g, 56.49 mmol) was added to the reaction mixture and the clear reaction mixture was vacuumed one more time and filled with N_2. The above mixture was cooled to 0 ^{o}C in an ice bath and t-butyldimethylsilylchloride (5.08 g, 33.69 mmol) was added to the reaction mixture. The ice bath was removed after 1 hour and the resulting mixture was stirred at room temperature under N_2 for 18 hours. After completion of reaction, the reaction mixture was partitioned between ethyl acetate and water. Collected organic layer was washed with water, brine solution and dried over anhydrous Na_2SO_4. After evaporation, the product was purified by column chromatography (Si-gel, Hex: EtOAc = 5:1) and obtained as white foam. Yield: 96% (6.35 g). IR (KBr)ν̃3457, 3184, 3062, 2954, 2931, 2857,1694, 1607cm^{-1};^{1}H NMR ($CDCl_3$, 600 MHz): δ 8.96 (s, 1H), 8.07 (s, 1H), 6.26 (t, *J* = 6.6 Hz, 1H), 4.38 (s, 1H), 3.97 (s, 1H), 3.88 (d, *J* = 11.4 Hz, 1H), 3.75 (d, *J* = 10.8 Hz, 1H), 2.31-2.28 (m, 1H), 2.00-1.96 (m, 1H), 0.93 (s, 9H), 0.88 (s, 9H), 0.14 (d, *J* = 6.6 Hz, 6H), (0.07) (d, *J* = 4.8 Hz, 6H); ^{13}C NMR ($CDCl_3$, 150 MHz): δ 160.2, 150.0, 144.6, 88.6, 86.0, 72.7, 68.5, 63.2, 42.2,

38.7, 26.3, 25.9, 18.7, 18.2, -4.4, -4.6, -4.9, -5.0. **+ESI-HRMS** calculated for $C_{21}H_{40}IN_2O_5Si_2$**[M+H]**$^+$583.1515, found 583.1511.

Synthesis of3',5'-di-O-tert-butyldimethylsilyl-5-(3-((4-ethynylphenyl)(methyl)amino)propynyl)-2'-deoxyuridine (7): This compound was synthesised following a modified literature procedure. [44b]1.12 g (1.92 mmol) of 3',5'-bis-*O*-tert-butyldimethylsilyl-5-iodo-2'-deoxyuridine (**6**) and*N*-methyl-*N*-(prop-2-yn-1-yl)-4-((trimethylsilyl)ethynyl)aniline (**4**) were taken in a dry R.B. and dissolved in 15 ml dry Et_3N. The resulting mixture was degassed by bubbling N_2 through it. After 10 minutes, $PdCl_2(PPh_3)_2$ (40.49 mg, 0.057 mmol) followed by CuI (3.66 mg, 0.019 mmol) were added to the above mixture while continuing the degassing. The resulting mixture was stirred at 55 °C for 7 h. After completion, the reaction mixture was partitioned between ethyl acetate and water. Collected organic layer was washed with aqueous ammonium chloride, water, brine solution and dried over anhydrous Na_2SO_4. After evaporation, the product was purified by column chromatography (Si-gel, Hex: EtOAc = 3:1) and obtained as light brown foam. Yield: 78 % (783 mg). IR (KBr)ṽ3451, 3047, 2954, 2930, 1714, 1688, 1609 cm^{-1}; ^{1}H NMR ($CDCl_3$, 600 MHz) δ 8.53 (s, 1H), 7.86 (s, 1H), 7.35 – 7.32 (m, 2H), 6.72 – 6.69 (m, 2H), 6.25 (dd, J = 7.5, 5.4 Hz, 1H), 4.38-4.36 (m, 1H), 4.25 (s, 2H), 3.96 (q, J = 2.4 Hz, 1H), 3.84 (dd, J = 11.4, 2.4 Hz, 1H), 3.73 (dd, J = 11.4, 2.4 Hz, 1H), 3.01 (s, 3H), 2.31 – 2.27 (m, 1H), 2.00 – 1.96 (m, 1H), 0.88 (s, 9H), 0.87 (s, 9H), 0.22 (s, 9H), 0.07 (s, 3H), 0.06 (s, 6H), 0.04 (s, 3H); ^{13}C NMR ($CDCl_3$, 150 MHz) δ 161.5, 149.2, 148.9, 142.4, 133.3, 113.1, 111.7, 106.3, 99.8, 91.7, 89.7, 88.5, 86.0, 77.2, 75.3, 72.6, 63.1, 43.0, 42.1, 38.4, 26.1, 25.8, 18.5, 18.1, 0.3, -4.5, -4.7, -5.2, -5.5. **+ESI-HRMS** calculated for $C_{36}H_{58}N_3O_5Si_3$**[M+H]**$^+$696.3679, found 696.3672.

Synthesis of3',5'-di-O-tert-butyldimethylsilyl-5-(3-((4-ethynylphenyl)(methyl)amino)propynyl)-2'-deoxyuridine(8): This compound was synthesised following a modified literature procedure.[44c] 991 mg (1.42 mmol) of **(7)** was taken

in a dry R.B. and dissolved in 10 ml drymethanol. Anhydrous K_2CO_3 (984g, 7.11 mmol) was added to the above solution and the resulting mixture was stirred for 4 hours at room temperature. After completion of reaction, the reaction mixture was partitioned between ethyl acetate and water. Collected organic layer was washed with water, brine solution and dried over anhydrous Na_2SO_4. After evaporation, the product was purified by column chromatography (Si-gel, Hex: EtOAc = 4:1) and obtained as dark orange foam. Yield: 87% (773g). IR (KBr) $\tilde{\nu}$ 3312, 2954, 2928, 1712, 1685, 1609 cm^{-1}; ^1H NMR ($CDCl_3$, 600 MHz):δ 9.23 (s, 1H), 7.86 (s, 1H), 7.36 (d, *J* = 8.4 Hz, 2H), 6.72 (d, *J* = 9.0 Hz, 2H), 6.25 (t, *J* = 6.6 Hz, 2H), 4.36 (t, *J* = 2.4 Hz, 1H), 3.95 (s, 1H), 3.83 (d, *J* = 11.4 Hz, 1H), 3.72 (d, *J* = 11.4, 1H), 3.01 (s, 3H), 2.96 (s, 1H), 2.31-2.28 (m, 1H), 2.00-1.92 (m, 1H), 0.87 (s, 9H), 0.86 (s, 9H), 0.06 (s, 6H), 0.03 (s, 6H); **+APCI-HRMS** calculated for $C_{33}H_{50}N_3O_5Si_2$**[M+H]**$^+$ 624.3284, found 624.3299.

General Procedure for the synthesis of Aryl Azides: An ice cold solution of sodium nitrite (3 eqv.) in water was added dropwise to a cold solution of aryl amine (1 eqv.) in water and concentrated hydrochloric acid at 0 °C over 7 to10 min. The reaction mixture was slowly stirred for 1-2 min before an ice cold solution of sodium azide (6 eqv.) in water was added dropwise at 0 °C over 10 min. The mixture was stirred for 15 min. The resulting mixture was extracted with hexane. The organic layer was washed with water, followed by a brine solution, dried over anhydrous Na_2SO_4. After evaporation, the product was passed through a section of silica gel (60-120 mesh). Formation of the azides was confirmed from IR study and yields were within 60%-80% in all cases. The produced azides were then immediately used for the next step without further purification.

General Procedure for Click Reaction: Alkyne (1 eqv.) and azide (1.5 eqv.) were suspended in a 1:1 water/*tert*-butanol mixture. Sodium ascorbate (0.05 eqv., freshly prepared in 1ml water) was added, followed by $CuSO_4.5H_2O$ (0.2eqv., freshly prepared in 1ml water).

The reaction mixture was refluxed (75 °C) for 12 hours. The progress of the reaction was monitored by TLC. After completion of reaction, *tert*-butanol was evaporated in rotary evaporator and the reaction mixture was partitioned between ethyl acetate and water. Collected organic layer was washed with water, aqueous ammonium chloride, brine solution and dried over anhydrous Na_2SO_4. After evaporation, the product was purified by column chromatography.

General Procedure for deprotection of tertiarybutyldimethylsilyl ether: To a solution of respective TBDMS protected nucleoside (1eqv.) in THF, a solution of tetra-*n*-butylammoniumfluoride (TBAF) (2.5 eqv.) in THF was added. The reaction mixture was stirred at room temperature for 1 hour. After completion of reaction, solvent was evaporated in rotary evaporator and was partitioned between ethyl acetate and water. Collected organic layer was washed with brine solution and dried over anhydrous Na_2SO_4. After evaporation, the crude material obtained was purified by column chromatography.

Synthesis of 3',5'-di-O-tert-butyldimethylsilyl-5-(3-((4-(1-(4-bromophenyl)-triazolyl)phenyl)(methyl)amino)propynyl)-2'-deoxyuridine (9A):Using general procedure for click reaction, starting from 100 mg (0.16 mmol) of compound **8** and 47.5 mg of 1-azido-4-bromobenzene (0.24 mmol), the title compound **9A** was isolated pure by Si-gel column chromatography (Hex: EtOAc = 3:1) as yellow solid. Yield: 52% (68 mg); m.p. 138-140 °C. IR (KBr)ṽ3423, 2928, 2856, 1717, 1688, 1618 cm^{-1}; ^1H NMR ($CDCl_3$, 600 MHz): δ 8.05 (s, 1H), 7.90 (s, 1H), 7.77 (d, *J* = 8.4 Hz, 2H), 6.90 (d, *J* = 8.4 Hz, 2H), 6.25 (t, *J* = 6.6 Hz, 2H), 4.36 (s,1H), 4.28 (s, 2H), 3.95 (s, 1H), 3.84 (d, *J* = 11.4 Hz, 1H), 3.72 (d, *J* = 11.4, 1H), 3.05 (s, 3H), 2.30-2.27 (m, 1H), 2.00-1.96 (m, 1H), 0.86 (s, 18H), 0.07 (s, 6H), 0.05 (s, 6H); ^{13}C NMR ($CDCl_3$, 150 MHz)δ 149.3, 149.1, 142.5, 136.3, 133.0, 122.2, 121.9, 119.7, 116.1, 114.1, 99.9, 90.1, 88.6,

86.1, 75.4, 72.6, 63.1, 43.3, 42.1, 38.7, 26.1, 25.9, –4.4, –4.6, –5.1, –5.4; **+ESI-HRMS** calculated for $C_{39}H_{54}BrN_6O_5Si_2$ **[M+H]**$^+$ 821.2872, found 821.2873.

Synthesis of 3',5'-di-O-tert-butyldimethylsilyl-5-(3-((4-(1-(4-nitrophenyl)-triazolyl)phenyl)(methyl)amino)propynyl)-2'-deoxyuridine(9B): Using general procedure for click reaction, starting from 100 mg (0.16 mmol) of compound **8** and 40 mg of 1-azido-4-nitrobenzene (0.24 mmol), the title compound **9B**was isolated pure pure by Si-gel column chromatography (Hex: EtOAc = 1:1) as rust brown solid. Yield: 52% (68 mg). IR (KBr)ῡ3427, 2925, 1688, 1618, 1501 cm^{-1}; ^{1}H NMR ($CDCl_3$, 600 MHz): δ 9.39 (s, 1H), 8.36 (d, *J* = 8.4 Hz, 2H), 8.18 (s, 1H), 7.97 (d, *J* = 8.4 Hz, 2H), 7.95 (s, 1H), 7.75 (d, *J* = 8.4 Hz, 2H), 6.88 (d, *J* = 8.4 Hz, 2H), 6.26 (t, *J* = 6 Hz, 1H), 4.37 (s,1H), 4.25 (s, 2H), 3.95 (s, 1H), 3.87 (d, *J* = 10.8 Hz, 1H), 3.74 (d, *J* = 11.4, 1H), 3.03 (s, 3H), 2.30-2.28 (m, 1H), 2.01-1.97 (m, 1H), 0.89 (s, 9H), 0.87 (s, 9H), 0.1 (s, 6H), 0.06 (s, 6H); ^{13}C NMR ($CDCl_3$, 150 MHz):δ 162.1, 149.6, 149.5, 149.4, 147.0, 142.6, 141.4, 127.1, 125.6, 120.2, 119.1, 116.0, 11 4.1, 99.9, 90.0, 88.6, 86.1, 75.7, 72.6, 63.1, 43.3, 42.2, 38.9, 26.2, 25.9, –4.5, –4.6, –5.2, –5.4 ; **+ESI-HRMS** calculated for $C_{39}H_{54}N_7O_7Si_2$ **[M+H]**$^+$ 788.3618, found 788.3617.

Synthesis of3',5'-di-O-tert-butyldimethylsilyl-5-(3-((4-(1-(4-cyanophenyl)-triazolyl)phenyl)(methyl)amino)propynyl)-2'-deoxyuridine(9C): Using general procedure for click reaction, starting from 100 mg (0.16 mmol) of compound **8** and 35 mg of 4-azidobenzonitrile (0.24 mmol), the title compound **9C** was isolated pure by Si-gel column chromatography (Hex: EtOAc = 2:1)as yellow solid. Yield: 94% (116 mg); m.p. 135-137 °C. IR (KBr)ῡ3415, 2929, 2857, 1699, 1619, 1607 cm^{-1}; ^{1}H NMR ($CDCl_3$, 600 MHz): δ 9.39 (s, 1H), 8.36 (d, *J* = 8.4 Hz, 2H), 8.18 (s, 1H), 7.97 (d, *J* = 8.4 Hz, 2H), 7.95 (s, 1H), 7.75 (d, *J* = 8.4 Hz, 2H), 6.88 (d, *J* = 8.4 Hz, 2H), 6.26 (t, *J* = 6 Hz, 1H), 4.37 (s,1H), 4.25 (s, 2H), 3.95 (s, 1H), 3.87 (d, *J* = 10.8 Hz, 1H), 3.74 (d, *J* = 11.4, 1H), 3.03 (s, 3H), 2.30-2.28 (m, 1H), 2.01-1.97 (m, 1H), 0.89 (s, 9H), 0.87 (s, 9H), 0.1 (s, 6H), 0.06 (s, 6H); ^{13}C NMR ($CDCl_3$, 150

MHz):δ 162.1, 149.6, 149.5, 149.4, 147.0, 142.6, 141.4, 127.1, 125.6, 120.2, 119.1, 116.0, 11 4.1, 99.9, 90.0, 88.6, 86.1, 75.7, 72.6, 63.1, 43.3, 42.2, 38.9, 26.2, 25.9, –4.5, –4.6, –5.2, –5.4 ;+**ESI-HRMS** calculated for $C_{40}H_{54}N_7O_5Si_2$**[M+H]**$^+$ 768.3719, found 768.3717.

Synthesis of3',5'-di-O-tert-butyldimethylsilyl-5-(3-(methyl(4-(1-(4-(trifluoromethyl)-7-coumarinyl)-triazolyl)phenyl)amino)propynyl)-2'-deoxyuridine(9D):Using general procedure for click reaction, starting from 100 mg (0.16 mmol) of compound **8** and 61 mg of 7-azido-4-trifluoromethylcoumarin (0.24 mmol), the title compound **9D** was isolated pure by Si-gel column chromatography (Hex: EtOAc =1:1)as yellow solid. Yield: 94% (132 mg); m.p. 227-230 °C. IR (KBr) ῡ3425, 2955, 2929, 1720, 1686, 1617, 1607 cm^{-1}; ^{1}H NMR ($CDCl_3$, 600 MHz): δ 8.97 (s, 1H), 8.17 (s, 1H), 7.92 (s, 1H), 7.85 (d, *J* = 12.6 Hz, 3H), 7.77 (d, *J* = 7.2 Hz, 2H), 6.89 (d, *J* = 6.6 Hz, 2H), 6.83 (s, 1H), 6.25 (t, *J* = 6.6 Hz, 2H), 4.37 (s,1H), 4.26 (s, 2H), 3.95 (s, 1H), 3.85 (d, *J* = 11.4 Hz, 1H), 3.73 (d, *J* = 10.8, 1H), 3.04 (s, 3H), 2.30-2.28 (m, 1H), 2.01-1.98 (m, 1H), 0.88 (s, 9H), 0.87 (s, 9H), 0.08 (s, 6H), 0.06 (s, 6H); 13C NMR (CDCl3, 150 MHz): δ 161.8, 158.34, 155.3, 149.6, 149.5, 149.3, 142.5, 140. 2, 127.1, 119.1, 116.4, 115.7, 114.1, 113.1, 108.5, 99.9, 89.9, 88.1, 75.6, 72.6, 63.16, 43.3, 42.2, 38.7, 29.8, 26.2, 25.9, 18.5, 18.2, -4.4, -4.6, -5.1, -5.4; **+ESI-HRMS** calculated for $C_{43}H_{54}F_3N_6O_7Si_2$**[M+H]**$^+$ 879.3539, found 879.3531.

Synthesis of3',5'-di-O-tert-butyldimethylsilyl-5-(3-((4-(1-(1-naphthyl)-triazolyl)phenyl)(methyl)amino)propynyl)-2'-deoxyuridine(9E)**:** Using general procedure for click reaction, starting from 104 mg (0.166 mmol) of compound **8** and 1-azidonaphthalene (42.25 mg, 0.25 mmol), the title compound **9F** was isolated pure by Si-gel column chromatography (Hex: EtOAc = 2:1)as brown semi-solid. Yield: 53% (70 mg); m.p. 91-94 °C. IR (KBr)ῡ3408, 2954, 2928, 2856, 1698, 1619 cm^{-1}; ^{1}H NMR ($CDCl_3$, 400 MHz): δ 8.95 (s, 1H), 8.03 (s, 2H), 7.96 (bs, 1H), 7.90 (s, 1H), 7.83 (bs, 2H), 7.69 (bs, 1H), 7.59 (m, 5H), 6.93 (bs, 2H), 6.25 (s, 1H), 4.37 (s, 1H), 4.29 (s, 2H), 3.95 (s, 1H), 3.84 (bs, 1H), 3.74-3.73 (m, 1H),

3.06 (s, 3H), 2.28-2.28 (m, 1H), 1.99 (bs, 1H), 0.87 (s, 18H), 0.06 (s, 12H); ^{13}C NMR ($CDCl_3$, 100 MHz): δ161.9,149.3, 148.2, 142.5, 134.3, 130.4, 128.8, 128.4, 127.2, 127.0, 125.2, 123.7, 122.7, 121 .2, 120.0, 114.2, 99.9, 90.1, 88.6, 86.1, 77.5, 77.2, 76.9, 75.3, 72.6, 63.1, 43.3, 42.1, 38.7, 26. 1, 25.9, –4.4, –4.6, –5.1, –5.4. **+ESI-HRMS** calculated for $C_{43}H_{57}N_6O_5Si_2$**[M+H]**$^+$ 793.3923, found 793.3925.

Synthesis of3',5'-di-O-tert-butyldimethylsilyl-5-(3-((4-(1-(2-anthrayl)-triazolyl)phenyl)(methyl)amino)propynyl)-2'-deoxyuridine(9F):Using general procedure for click reaction, starting from 100 mg (0.16 mmol) of compound **8** and 53 mg of 2-azidoanthracene (0.24 mmol), the title compound **9G** was isolated pure by Si-gel column chromatography (Hex: EtOAc = 3:1)as yellow solid. Yield: 57% (77 mg); m.p. 204-208 °C. IR (KBr)ῡ3406, 2953, 2928, 2856, 1699, 1619 cm^{-1}; ^{1}H NMR ($CDCl_3$, 600 MHz):δ 8.51 (s, 1H), 8.49 (s, 1H), 8.42 (s, 1H), 8.33 (s, 1H), 8.25 (s, 1H), 8.17 (d, *J* = 9.0 Hz, 1H), 8.03 (dd, *J* = 5.4, 3.6 Hz, 2H), 7.98 (dd, *J* = 9.0, 2.0 Hz, 1H), 7.91 (s, 1H), 7.84 (d, *J* = 8.4 Hz, 2H), 7.55 – 7.50 (m, 2H), 6.93 (d, *J* = 8.4 Hz, 2H), 6.25 (dd, *J* = 7.8, 6.0 Hz, 1H), 4.39 – 4.36 (m, 1H), 4.30 (s, 2H), 3.96 (d, *J* = 2.4 Hz, 1H), 3.85 (dd, *J* = 11.4, 2.4 Hz, 1H), 3.73 (dd, *J* = 11.4, 2.4 Hz, 1H), 3.07 (s, 3H), 2.31– 2.27 (m, 1H), 2.02 – 1.97 (m, 1H), 0.88 (s, 9H), 0.88 (s, 9H), 0.08 (d, *J* = 2.4 Hz, 6H), 0.06 (d, *J* = 4.8 Hz, 6H); ^{13}C NMR ($CDCl_3$, 150 MHz): δ 161.5, 149.3, 149.1, 142.4, 134.1, 132.6, 130.9, 130.7, 128.4, 128.2, 127.1, 127.0, 126.8, 126.4, 126.2, 119.9, 119.2, 117.8, 116.3, 114.1, 99.9, 88.5, 86.1, 77.1, 75.3, 72.6, 63.1, 43.3, 42.1, 38.7, 26.1, 25.8, 18.5, 18.1, -4.5, -4.7, -5.2, -5.46. **+ESI-HRMS** calculated for $C_{47}H_{59}N_6O_5Si_2$**[M+H]** $^+$ 843.4080, found 843.4085.

Synthesis of 3',5'-di-O-tert-butyldimethylsilyl-5-(3-((4-(1-(4-pyrenyl)-triazolyl)phenyl)(methyl)amino)propynyl)-2'-deoxyuridine (9G):Using general procedure for click reaction, starting from 100 mg (0.16 mmol) of compound **8** and 58 mg of 1-azidopyrene

(0.24 mmol), the title compound **9G** was isolated pure by Si-gel column chromatography (Hex: EtOAc = 3:1) as pale yellow solid. Yield: 77% (107 mg); m.p. 135-138 °C. IR (KBr)ῡ3423, 3046, 2954, 2928, 2856, 1699, 1619 cm^{-1}; ^{1}H NMR ($CDCl_3$, 600 MHz): δ 8.29 (dd, *J* = 6.0, 3 Hz, 2H), 8.26 (d, *J* = 6.6 Hz, 1H), 8.20 (d, *J* = 9.0 Hz, 1H), 8.16 (s, 1H), 8.16 (s, 1H), 8.14 (s, 1H), 8.13 – 8.08 (m, 2H), 7.96 (d, *J* = 9.0 Hz, 1H), 7.90 (d, *J* = 6.0 Hz, 2H), 7.88 (s, 1H), 6.96 (d, *J* = 9.0 Hz, 2H), 6.25 (dd, *J* = 7.8, 5.4 Hz, 1H), 4.38 (dt, *J* = 5.4, 2.4 Hz, 1H), 4.31 (s, 2H), 3.96 (q, *J* = 2.4 Hz, 1H), 3.86 (dd, *J* = 11.4, 2.4 Hz, 1H), 3.74 (dd, *J* = 11.4, 1.8 Hz, 1H), 3.08 (s, 3H), 2.32 – 2.27 (m, 1H), 2.03 – 1.97 (m, 1H), 0.90 (s, 9H), 0.88 (s, 9H), 0.09 (d, *J* = 3.0 Hz, 6H), 0.07 (d, *J* = 4.8 Hz, 6H); ^{13}C NMR ($CDCl_3$, 150 MHz) δ 161.4, 149.3, 149.1, 148.3, 142.4, 132.3, 131.3, 130.8, 130.8, 129.7, 129.0, 127.2, 127.1, 126.9, 126.5, 126.38, 126.2, 125.2, 124.9, 124.36, 123.5, 121.6, 121.5, 120.1, 114.2, 99.9, 90.1, 88.6, 86.1, 77.4, 77.1, 76.9, 75.3, 72.6, 63.1, 43.3, 42.1, 38.7, 26.1, 25.8, 18.5, 18.1, -4.5, -4.7, -5.2, -5.4. **+ESI-HRMS** calculated for $C_{49}H_{59}N_6O_5Si_2$**[M+H]** $^{+}$ 867.4080, found 867.4082.

Synthesis of5-(3-((4-(1-(4-cyanophenyl)-triazolyl)phenyl)(methyl)amino)propynyl)-2'-deoxyuridine (10C):Using general procedure for TBDMS deprotection, starting from 230 mg (0.3 mmol) of nucleoside **9C**, the title compound **10C** was isolated pure by Si-gel column chromatography ($CHCl_3$: MeOH = 10:1) as orange-yellow solid. Yield: 81% (130 mg); m.p. 178-181 °C. IR (KBr)ῡ3426, 3056, 2925, 2837, 2229, 1714, 1607, 1619 cm^{-1}; ^{1}H NMR (DMSO-d6, 600 MHz): δ 11.54 (s, 1H), 9.23 (s, 1H), 8.15 – 8.12 (m, 3H), 8.09 (d, *J* = 9.0 Hz, 2H), 7.74 (d, *J* = 9.0 Hz, 2H), 6.95 (d, *J* = 9.0 Hz, 2H), 6.04 (t, *J* = 6.6 Hz, 1H), 5.21 (d, *J* = 4.2 Hz, 1H), 5.06 (t, *J* = 5.0 Hz, 1H), 4.34 (s, 2H), 4.20 – 4.15 (m, 1H), 3.74 (q, *J* = 3.6 Hz, 1H), 3.59 – 3.53 (m, 1H), 3.54 – 3.49 (m, 1H), 2.95 (s, 3H); ^{13}C NMR (DMSO-d6, 150 MHz) δ 161.5, 149.4, 149.1, 148.3, 143.7, 139.6, 134.3, 126.4, 120.2, 118.8, 118.2, 117.9, 113.9, 110.8, 98.1, 88.6, 87.6, 84.8, 76.1, 70.1, 60.9, 42.1, 40.2, 40.1, 38.0. **+ESI-HRMS** calculated for $C_{28}H_{26}N_7O_5$**[M+H]**$^{+}$ 540.1990, found 540.1990.

***Synthesis of5-(3-((4-(1-(naphthayl)-triazolyl)phenyl)(methyl)amino)propynyl)-2'-deoxyuridine(10E*)**: Using general procedure for TBDMS deprotection, starting from 94 mg (0.12 mmol) of **(9E)**, the title compound was isolated pure by Si-gel column chromatography ($CHCl_3$: MeOH = 20:1)as pale yellow solid. Yield: 80% (53 mg); m.p. 152-155 °C. IR (KBr)ṽ3417, 3059, 2922, 2851, 1691, 1618cm^{-1}; ^{1}H NMR (600 MHz, DMSO-d6) δ 11.61 (s, 1H), 8.96 (s, 1H), 8.21 (d, *J* = 8.4 Hz, 1H), 8.18 (s, 1H), 8.14 (d, *J* = 7.8 Hz, 1H), 7.83 (d, *J* = 8.7 Hz, 2H), 7.80 (d, *J* = 7.0 Hz, 1H), 7.75 – 7.70 (m, 1H), 7.70 – 7.59 (m, 3H), 6.99 (d, *J* = 9.0 Hz, 2H), 6.08 (t, *J* = 6.6 Hz, 1H), 5.25 (d, *J* = 4.2 Hz, 1H), 5.12 (t, *J* = 5.0 Hz, 1H), 4.39 (s, 2H), 4.22 (p, *J* = 4.2 Hz, 1H), 3.78 (q, *J* = 3.2 Hz, 1H), 3.63 – 3.58 (m, 1H), 3.58 – 3.53 (m, 1H), 2.99 (s, 3H); ^{13}C NMR (DMSO-d6, 150 MHz) δ 172.2, 161.6, 149.5, 148.9, 147.1, 143.7, 133.7, 133.5, 130.2, 128.4, 128.1, 127.9, 127.2, 126.4, 125.5, 123.8, 122.6, 122.2, 119.5, 114.1, 98.2, 88.7, 87.6, 84.8, 79.2, 76.2, 70.1, 60.9, 45.7, 42.3, 40.2, 40.1, 38.1. **+ESI-HRMS** calculated for $C_{31}H_{29}N_6O_5$**[M+H]**$^+$ 565.2194 , found 565.2203.

Synthesis of5-(3-((4-(1-(pyrenyl)-triazolyl)phenyl)(methyl)amino)propynyl)-2'-deoxyuridine (10G):Using general procedure for TBDMS deprotection, starting from 158 mg (0.18 mmol) of **(9G)**, the title compound was isolated pure by Si-gel column chromatography ($CHCl_3$: MeOH = 20:1)as light brown solid. Yield: 85% (99 mg); m.p. 217-220 °C. IR (KBr)ṽ3420, 3054, 2924, 2851, 1691, 1618cm^{-1}; ^{1}H NMR (DMSO-d6, 600 MHz): δ 11.60 (s, 1H), 9.10 (s, 1H), 8.52 (d, *J* = 8.4 Hz, 1H), 8.46 (d, *J* = 7.2 Hz, 1H), 8.42 (d, *J* = 7.8 Hz, 1H), 8.40 – 8.33 (m, 3H), 8.30 (d, *J* = 9.0 Hz, 1H), 8.22 – 8.17 (m, 2H), 7.93 – 7.87 (m, 3H), 7.01 (d, *J* = 8.4 Hz, 2H), 6.09 (t, *J* = 6.6 Hz, 1H), 5.25 (d, *J* = 4.2 Hz, 1H), 5.12 (t, *J* = 4.8 Hz, 1H), 4.40 (s, 2H), 4.22 (p, *J* = 4.2 Hz, 1H), 3.79 (q, *J* = 3.6 Hz, 1H), 3.64 – 3.59 (m, 1H), 3.59 – 3.54 (m, 1H), 3.01 (s, 3H).^{13}C NMR (DMSO-d_6, 150 MHz) δ 161.6, 149.5, 148.9, 147.3, 143.7, 131.7, 130.7, 130.5, 130.2, 129.7, 128.86, 127.2, 127.2, 126.6, 126.4, 126.2, 125.4, 125.2, 124.1, 123.8, 123.4, 123.0, 121.2, 119.5, 114.1, 98.2, 88.7, 87.6, 84.8, 79.2, 76.2, 70.1, 60.9,

42.3, 40.1, 40.1, 39.5, 38.1. **+ESI-HRMS** calculated for $C_{37}H_{31}N_6O_5$**[M+H]**$^+$ 639.2350, found 639.2313.

UV-Visible Measurements: All the *UV* –visible spectra for the nucleosides (10 μM) were measured in different solvents using a UV-Visible spectrophotometer with a cell of 1 cm path length.

Fluorescence Experiments: All the sample solutions were prepared and used immediately. Fluorescence spectra were obtained using a fluorescence spectrophotometer at 25 °C using 1 cm path length cell. The fluorescence quantum yields (Φ_f) were determined using quinine sulphate as a reference with the known Φ_f (0.55) in 0.1 molar solution in sulphuric acid.

Fluorescence Lifetime Measurements: Fluorescence lifetimes were measured with the use of a system that employs microchannel plate photomultiplier as detector. Edinburgh 290 nm, 308 nm Pulsed LED and 375 nm Laser Diode were used wherever applicable for excitation. The fluorescence decay was analyzed by reconvolution and/or tail fitting method using in built software. All experiments were performed at 298 K.

Theoretical Calculation: The ground state structures of the fluorophores were optimized using density functional theory (DFT)[28] with B3LYP functional and 6-31G (d) basis set. The excited state related calculations were carried out with the Time dependent density functional theory (TD-DFT) with the optimized structure of the ground state (B3LYP/6-31G(d)). There are no imaginary frequencies in frequency analysis of all the calculated structures, therefore each calculated structure is a local energy minimum.

Studies on the Interaction of Pyrenyl nucleoside with BSA

***Preparation of BSA solution*:** Phosphate buffer of pH 7.02 was used to prepare the solution of BSA (Merck). A 1200 μM of stock BSA solution was prepared by dissolving 0.08 gm of BSA in 1 mL phosphate buffer (20 mM) of pH 7.0. From that stock solution sub stock of 1000 μM BSA was prepared. The compound stock solution was prepared in DMF because of the poor solubility in water. 1.0 mg of nucleoside was dissolved in 1.5 mL DMF to make a stock probe solution of concentration 910.3 μM.

***General experimental on interaction study of BSA by photophysical study*:** All the spectral measurements were carried out at room temperature. To study the interaction of compound with BSA, an aqueous solution of nucleoside (10 μM) was titrated with different concentrations of BSA (ranging from 0, 0.25, 0.5, 7.5, 1.0, 1.5, 2, 2.5, 3.0, 4, 5, 6, 10, 14, 18, 20 equivalent). The total volume of the final solution for each sample was 3 mL. The % of DMF content was 2%. The presence of 2% DMF does not induce structural changes to biomolecules. Each sample solution was mixed well before spectral measurements.

***UV-Visible study with BSA*:**The UV–Visible absorbance measurements were performed using UV-visible spectrophotometer with a cell of 1 cm path length at 298 K. All the UV-Visible studies were carried out in 20 mM phosphate buffer of pH 7.02 containing solution at 298 K. 2 % DMF was used to solubilize the probe. The measurements were taken in absorbance mode and the absorbance values of the sample solutions were measured in the wavelength regime of 200– 700 nm. All the experiments were carried out with freshly prepared sample solutions.

Fluorescence study with BSA:All fluorescence and steady state anisotropy experiments were performed using a steady state fluorescence spectrophotometer with a cell of 1 cm path length at 298 K. The excitation wavelength for probe nucleoside was set at 220 nm, 420 nm and emission spectra were measured in the wavelength regime of 290–650 nm. Steady state

anisotropy of the solutions was measured using steady state fluorescence spectrophotometer. The fluorescence lifetime experiment was carried out as described above.

Molecular Docking

Docking calculations were carried out using Autodock 4.2.[45] The amino acid sequence of BSA protein was observed from the NCBI website, http://www.ncbi.nlm.nih.gov/protein/CAA76847.1 The 3D model of the BSA protein was built using the 3D structure 1AO6 chain 'A' as template using the ESyPred3D11 web server. This template shares 72.4% identities with the BSA sequence. [>gi|3336842|emb|CAA76847.1| bovine serum albumin [Bos taurus]. To test accuracy of the docking results, the docking process was repeated three times. The AutoDock tools (ADT) were utilised for charges and polar hydrogens addition as well as for setting the other parameters. AutoGrid 4.0 and AutoDock 4.0 were used to produce grid maps. A grid box to a size of 126 × 126 × 126 with 0.378 Å spacing was generated. Total grid points per map were 2048383. The centre grid box for x-, y- and z centres were 37.396, 30.567 and 98.389 with offsets 2.528,6.528 and -0.389, respectively.In the prescriptive grid box, we calculated the complex conformation with flexible molecular docking method. The Lamarckian genetic algorithm (LGA) [45a] was choosen to carry out a flexible molecular docking of the small molecules to the receptor and to calculate the complex conformation. The other items used were the default settings. A total of 10 conformations from each docking were obtained and the least binding energy was considered as the best-docked conformation. Further intermolecular-hydrophobic, polar and hydrogen bond interactions were analysed using PyMOL[46a-b] and online protein-ligand interaction profilier[46c-d] (PLIP).

Supporting Information Available: Photophysical spectra, Cartesian coordinates, TDDFT calculation, ^{1}H /^{13}C NMR spectra. This material is available free of charge via the Internet at http://pubs.acs.org.

ACKNOWLEDGMENTS: This work is dedicated to Professor Amit Basak (IIT Kharagpur) on his 67th birth day. The authors thank DBT, [BT/PR5169/BRB/10/1065/2012 and BT/PR5169/ BMB/2015/39] Govt. of India., for financial support. H. G. thanks IIT Guwahati for a fellowship.

REFERENCES

1. (a) Loving, G. S.; Sainlos, M.; Imperiali, B. Monitoring protein interactions and dynamics with solvatochromic fluorophores. *Trends Biotechnol.* **2010**, *28*, 73. (b) Amaro, M.; Šachl, R.; Jurkiewicz, P.; Coutinho, A.; Prieto, M.; Hof, M. Time-Resolved Fluorescence in Lipid Bilayers: Selected Applications and Advantages over Steady State. *Biophys. J.* **2014**, *107*, 2751. (c) Wu, F.-Y.; Xiang. Y.-L.; Wu, Y.-M; Xie, F.-Y. *J.* Study of interaction of a fluorescent probe with DNA. *Luminescence* **2009**, *129*, 1286.
2. (a) McCarthy,J. J.; Hilfiker, R. The use of single-nucleotide polymorphism maps in pharmacogenomics. *Nat. Biotech.* **2000**, *18*, 505. (b) Okamoto, A.; Kanatani, K.; Saito, I. Pyrene-Labeled Base-Discriminating Fluorescent DNA Probes for Homogeneous SNP Typing. *J. Am. Chem. Soc.* **2004**, *126*, 4820. (c) Sholokh, M.; Improta, R.; Mori, M.; Sharma, R.; Kenfack, C.; Shin, D.; Voltz, K.; Stote, R. H.; Zaporozhets, O. A.; Botta, M.; Tor,Y.; Mély, Y. Tautomers of a Fluorescent G Surrogate and Their Distinct Photophysics Provide Additional Information Channels. *Angew.Chem. Int. Ed.* **2016**, *55*, 7974.
3. For reviews see: (a) Sinkeldam, R. W.; Greco,N. J.; Tor, Y. Fluorescent Analogs of Biomolecular Building Blocks: Design, Properties and Applications. *Chem. Rev.* **2010**,

110, 2579. (b) Wilson, J. N.; Kool, E. T. Fluorescent DNA base replacements: Reporters and sensors for biological systems. *Org. Biomol. Chem.* **2006**, *4*, 4265. (c) Su, X.; Xiao, X.; Zhang,C.; Zhao, M. Nucleic acid fluorescent probes for biological sensing. *Appl. Spectrosc*. **2012**, *66*, 1249. (d) Dodd, D. W.; Hudson, R. H. E. Intrinsically Fluorescent Base-Discriminating Nucleoside Analogs. *Mini-Rev. Org. Chem.* **2009**, *6*, 378. (e) Wilhelmsson, L. M. Q. *Fluorescent nucleic acid base analogues. Rev. Biophys*. **2010**, *43*, 159.

4. Wilhelmsson, L. M. Fluorescent nucleic acid base analogues. *Quart. Rev. Biophys.* **2010**, **43**, 159.
5. (a) Wilson, J. N.; Kool, E. T. Fluorescent DNA base replacements: reporters and sensors for biological systems. *Org. Biomol. Chem.* **2006**, *4*, 4265. (b) Tanpure, A. A.;Pawar ,M. G.;Srivatsan, S. G. Fluorescent Nucleoside Analogs: Probes for Investigating Nucleic Acid Structure and Function. *Isr. J. Chem*. **2013**, *53*, 366. (c) Dziuba, D.; Pohl,R.; Hocek, M. Polymerase synthesis of DNA labelled with benzylidene cyanoacetamide-based fluorescent molecular rotors: fluorescent light-up probes for DNA-binding proteins. *Chem. Commun.* **2015**, *51*, 4880. (d) Kanamori, T.; Ohzeki, H.; Masaki, Y.; Ohkubo, A.; Takahashi, M.; Tsuda, K.; Ito, T.; Shirouzu, M.; Kuwasako, K.; Muto, Y.;Sekine,M.; Seio, K. Controlling the Fluorescence of Benzofuran-Modified Uracil Residues in Oligonucleotides by Triple-Helix Formation. *ChemBioChem.* **2015**, *16*, 167. (e) Tokugawa, M.; Masaki, Y.; Cauggadibrata, *J*. C.; Kaneko, K.; Shiozawa, T.; Kanamori, T.; Grotli, M.; Wilhelmsson, L. M.; Sekine,M.; Seio, K. 7-(Benzofuran-2-yl)-7-deazadeoxyguanosine as a fluorescence turn-ON probe for single-strand DNA binding protein. *Chem. Commun.* **2016**, *52*, 3809.
6. (a) Holzhauser, C.; Wagenknecht, H.-A. In-Stem-Labeled Molecular Beacons for Distinct Fluorescent Color Readout. *Angew. Chem., Int. Ed.* **2011**, *50*, 7268. (b) Guo,

J.; Ju, J.; Turro, N. J. Fluorescent hybridization probes for nucleic acid detection. *Anal. Bioanal. Chem.* **2012**, *402*, 3115.

7. (a) Furukawa, K.; Hattori, M.; Ohki, T.; Kitamura, Y.;Kitade,Y.; Ueno,Y. Nucleic acid probe containing fluorescent tricyclic base-linked acyclonucleoside for detection of single nucleotide polymorphisms. *Bioorg. Med. Chem.* **2012**, *20*, 16. (b) Kolpashchikov, D. M. Binary probes for nucleic acid analysis. *Chem. Rev.* **2010**, 110, 4709. (c) Okamoto, A.; Tainaka, K.; Saito, I. Clear Distinction of Purine Bases on the Complementary Strand by a Fluorescence Change of a Novel Fluorescent Nucleoside. *J. Am. Chem. Soc.* **2003**, *125*, 4972.
8. (a) Dai, N.; Kool, E. T. Fluorescent DNA-based enzyme sensors. *Chem. Soc.Rev.* **2011**, *40*, 5756. (b) Riedl, J.; Menova, P.; Pohl, R.; Orsag, P.; Fojta, M.; Hocek, M. GFP-like Fluorophores as DNA Labels for Studying DNA–Protein Interactions. *J.Org. Chem.* **2012**, *77*, 8287. (c) Riedl, J.; Pohl, R.; Ernsting, N. P.; Orsag, P.; Fojta, M. Labelling of nucleosides and oligonucleotides by solvatochromic 4-aminophthalimide fluorophore for studying DNA–protein interactions. *Chem. Sci.* **2012**, *3*,2797.
9. (a) Greco,N. *J.*; Tor, Y. Simple Fluorescent Pyrimidine Analogues Detect the Presence of DNA Abasic Sites. *J. Am. Chem. Soc.* **2005**, *127*, 10784. (b) Kanamori, T.; Ohzeki, H.; Masaki, Y.; Ohkubo, A.; Takahashi, M.; Tsuda, K.; Ito, T.;Shirouzu, M.; Kuwasako, K.; Muto, Y.; Sekine, M.; Seio, K. Controlling the Fluorescence of Benzofuran-Modified Uracil Residues in Oligonucleotides by Triple-Helix Formation. *ChemBioChem.* 2**015**, *16*, 167. (c) Saito, Y.; Suzuki, A.; Okada, Y.; Yamasaka, Y.; Nemoto,N.;Saito, I. An environmentally sensitive fluorescent purine nucleoside that changes emission wavelength upon hybridization. *Chem. Commun.* **2013**, *49*, 5684.
10. (a) Weber, G.; Farris, F. J. Synthesis and spectral properties of a hydrophobic fluorescent probe: 6-propionyl-2-(dimethylamino)naphthalene. *Biochemistry* **1979**, *18*,

3075. (b) Tainaka, K.; Tanaka, K.; Ikeda, S.; Nishiza, K.-i.; Unzai, T.; Fujiwara, Y.; Saito, I.; Okamoto, A. PRODAN-Conjugated DNA: Synthesis and Photochemical Properties. *J. Am. Chem. Soc.* **2007**, *129*, 4776.

11. Weinberger, M.; Berndt, F.; Mahrwald, R.; Ernsting,N. P.; Wagenknecht, H.-A. Synthesis of 4-Aminophthalimide and 2,4-Diaminopyrimidine C-Nucleosides as Isosteric Fluorescent DNA Base Substitutes. *J. Org. Chem.* **2013**, *78*, 2589.
12. Okamoto, A.; Tainaka, K.; Fujiwara, Y. Nile Red Nucleoside: Design of a Solvatofluorochromic Nucleoside as an Indicator of Micropolarity around DNA. *J. Org. Chem.* **2006**, *71*, 3592.
13. (a) Shinohara, Y.; Matsumoto, K.; Kugenuma, K.; Morii, T.; Saito ,Y.; Saito, I. Design of environmentally sensitive fluorescent 2′-deoxyguanosine containing arylethynyl moieties: Distinction of thymine base by base-discriminating fluorescent (BDF) probe. *Bioorg. Med. Chem. Lett.* **2010**, *20*, 2817. (b)Saito, Y.; Suzuki, A.; Okada, Y.; Yamasaka, Y.; Nemoto, N.; Saito, I. An environmentally sensitive fluorescent purine nucleoside that changes emission wavelength upon hybridization. *Chem. Commun.* **2013**, *49*, 5684. (c) Suzuki, A.; Saito, M.; Katoh, R.; Saito, Y. Synthesis of 8-aza-3,7-dideaza-2′-deoxyadenosines possessing a new adenosine skeleton as an environmentally sensitive fluorescent nucleoside for monitoring the DNA minor groove. *Org. Biomol. Chem.* **2015**, *13*, 7459.
14. Dziuba, D.; Pospíšil, P.; Matyašovský, J.; Brynda, J.; Nachtigallová, D.; Rulíšek, L.; Pohl, R.; Hof, M.; Hocek, M. Solvatochromic fluorene-linked nucleoside and DNA as color-changing fluorescent probes for sensing interactions. *Chem. Sci.* **2016**, ***7***, 5775.
15. (a) Demchenko, A. P. The concept of λ-ratiometry in fluorescence sensing and imaging. *J. Fluoresc.* **2010**, *20*, 1099. (b) Demchenko, A. P. Practical aspects of wavelength ratiometry in the studies of intermolecular interactions. *J. Mol. Struct.* **2014**, *1077*, 51.

(c) Xu, L.; He, M.-L.; Yang, H.-B.; Qian, X. A simple fluorescent probe for Cd2+ in aqueous solution with high selectivity and sensitivity. *Dalton Trans.* **2013**, *42*, 8218.

16. (a) Nandhikonda, P.; Heagy, M. D. Dual Fluorescent N-Aryl-2,3- naphthalimides: Applications in Ratiometric DNA Detection and White Organic Light-Emitting Devices. *Org. Lett.* **2010**, *12*, 4796. (b) Srikun, D.; Miller, E. W.; Domaille, D. W.; Chang, C. J. An ICT-Based Approach to Ratiometric Fluorescence Imaging of Hydrogen Peroxide Produced in Living Cells. *J. Am. Chem. Soc.* **2008**, *130*, 4596.
17. (a) Socher, E.; Bethge, L.; Knoll, A.; Jungnick, N.; Herrmann, A.; Seitz, O. Low-noise stemless PNA beacons for sensitive DNA and RNA detection. *Angew. Chem., Int. Ed.* **2008**, *47*,9555. (b) Teo,Y. N.;Kool, E. T. DNA-Multichromophore Systems. *Chem. Rev.***2012**, *112*, 4221.
18. (a) Lippert, E.; Lu¨der, W.; Boss, H. In *Advances in Molecular Spectroscopy*; Marngini, A., Ed.; Pergamon Press: Oxford, **1962**; p 443. (b) Weigel, W.; Rettig, W.; Dekhtyar, M.; Modrakowski, C.; Beinhoff, M.; Schlu¨ter, A. D. Dual Fluorescence of Phenyl and Biphenyl Substituted Pyrene Derivatives. *J. Phys. Chem. A* **2003**, *107*, 5941. (c) Rettig, W. Charge Separation in Excited States of Decoupled Systems—TICT Compounds and Implications Regarding the Development of New Laser Dyes and the Primary Process of Vision and Photosynthesis. *Angew. Chem., Int. Ed. Engl.* **1986**, *25*, 971. (d) Grabowski, Z. R.; Rotkiewicz, K.; Rettig, W. Structural Changes Accompanying Intramolecular Electron Transfer: Focus on Twisted Intramolecular Charge-Transfer States and Structures. *Chem. Rev.* **2003**, *103*, 3899.
19. (a) Okamoto, A.; Tainaka, K.; Nishiza, K.-i.;Saito, I. Monitoring DNA Structures by Dual Fluorescence of Pyrene Derivatives. *J. Am. Chem. Soc.* **2005**, *127*, 13128. (b) Dziuba, D.; Postupalenko, V. Y.; Spadafora, M.; Klymchenko, A. S.; Guérineau, V.; Mély, Y.; Benhida, R.; Burger, A. A Universal Nucleoside with Strong Two-Band

Switchable Fluorescence and Sensitivity to the Environment for Investigating DNA Interactions. *J. Am. Chem. Soc.* **2012**, *134*, 10209. (c) Gavvala, K.; Barthes, N. P. F.; Bonhomme, D.; Dabert-Gay, A. S.; Debayle, D.; Michel, B. Y.; Burger, A.; Mély, Y. A turn-on dual emissive nucleobase sensitive to mismatches and duplex conformational changes. *RSC Adv*ances, **2016**, ***6***, 87142. (d) Barthes, N. P. F.; Karpenko, I. A.; Dziuba, D.; Spadafora, M.; Auffret, J.; Demchenko, A. P.; M´ely, Y.; Benhida, R.; Michel, B. Y.; Burger, A. Development of environmentally sensitive fluorescent and dual emissive deoxyuridine analogues. *RSC Adv.* **2015**, *5*, 33536.

20. (a) Bag, S. S.; Saito, I. *In Fluorescent Analogues of Biomolecular Building Blocks: Design and Applications,* Eds., Tor, Yitzhak; Wilhelmsson, Marcus. Publisher: John Wiley & Sons (**2016**) ch 7, p-137-173.(b) Bag, S. S.; Kundu, R.; Matsumoto, K, Saito, Y.; Saito, I. Singly and doubly labeled base-discriminating fluorescent oligonucleotide probes containing oxo-pyrene chromophore. *Bioorg. Med.Chem. Lett.* **2010**, *20*, 3227. (c) Ensslen, P.; Gärtner, S.; Glaser, K.; Colsmann, A.; Wagenknecht, H.-A. A DNA-Fullerene Conjugate as a Template for Supramolecular Chromophore Assemblies: Towards DNA-Based Solar Cells. *Angew. Chem. Int. Ed*. **2016**, *55*, 1904. (d) Dziuba, D.; Pohla, R.; Hocek, M. Polymerase synthesis of DNA labelled with benzylidene cyanoacetamide-based fluorescent molecular rotors: fluorescent light-up probes for DNA-binding proteins. *Chem. Commun.* **2015**, *51*, 4880. (e) Liang, Y.; Gloudeman, *J.*; Wnuk, S. F. Palladium-Catalyzed Direct Arylation of 5-Halouracils and 5-Halouracil Nucleosides with Arenes and Heteroarenes Promoted by TBAF. *J. Org. Chem.* **2014**, *79*, 4094. (f) Saito, Y.; Bag, S. S.; Kusakabe, Y.; Nagai, C.; Matsumoto, K.; Mizuno, E.; Kodate, S.; Suzuka, I.; Saito, I. Dual-labeled oligonucleotide probe for sensing adenosinevia FRET: A novel alternative to SNPs genotyping. *Chem. Commun.* **2007**, *21*, 2133.(g) Bandy, T. *J.*; Brewer, A.; Burns, *J.* R.; Marth, G.; Nguyen, T. N.;

Stulz, E. DNA as supramolecular scaffold for functional molecules: progress in DNA nanotechnology. *Chem. Soc. Rev*. **2011**, *40*, 138.

21. (a) Bag, S. S.; Pradhan, M. K.; Das, S. K.; *J*ana, S.; Bag, R. Wavelength shifting oligonucleotide probe for the detection of adenosine of a target DNA with enhanced fluorescence signal. *Bioorg. Med. Chem. Lett.* **2014**, *24*, 4678. (b) Bag, S.S.; Talukdar, S.; Anjali, S.J. Regioselective and stereoselective route to N2-β-tetrazolyl unnatural nucleosides via SN2 reaction at the anomeric center of Hoffer's chlorosugar. *Bioorg. Med. Chem. Lett.* **2016**, *26*, 2044. (c) Bag, S.S.; Talukdar, S.; Matsumoto, K.; Kundu, R. Triazolyl Donor/Acceptor Chromophore Decorated Unnatural Nucleosides and Oligonucleotides with Duplex Stability Comparable to That of a Natural Adenine/Thymine Pair. *J. Org. Chem.*, **2013**, *78*, 278. (d) Bag, S. S.; Talukdar, S.; Kundu, R.; Saito, I.; *J*ana, S. Dual door entry to exciplex emission in a chimeric DNA duplex containing non-nucleoside–nucleoside pair. *Chem. Commun.* **2014**, *50*, 829.
22. (a) Meščić, A.; Harej, A.; Klobučar, M.; Glavač, D.; Cetina, M.; Pavelić, S. K.; Raić-Malić, S. Discovery of New Acid Ceramidase-Targeted Acyclic 5-Alkynyl and 5-Heteroaryl Uracil Nucleosides. *ACS Med. Chem. Lett*. **2015**, *6*, 1150. (b) Ingale, S. A.; Leonard, P.; Yanga, H.; Seela, F. 5-Nitroindole oligonucleotides with alkynyl side chains: universal base pairing, triple bond hydration and properties of pyrene "click" adducts. *Org. Biomol. Chem*. **2014**, *12*, 8519. (c) Agrofoglio, L. A.; Gillaizeau, I.; Saito, Y. Palladium-Assisted Routes to Nucleosides. *Chem. Rev*. **2003,** *103*, 1875. (d) Barnes, T. W.; Turner, D. H. Long-Range Cooperativity in Molecular Recognition of RNA by Oligodeoxynucleotides with Multiple C5-(1-Propynyl) Pyrimidines. *J. Am. Chem. Soc.* **2001**, *123*, 4107. (e) Wagner, R. W.; Matteucci, M. D.;Lewis, *J*. G.;Gutierrez, A. *J*.;Moulds, C.;Froehler, B. C. Antisense gene inhibition by oligonucleotides containing C-5 propyne pyrimidines. *Science* **1993**, *260*, 1510. (f) Seela, F.; Shaikh, K. I.

Oligonucleotides containing 7-propynyl-7-deazaguanine: synthesis and base pair stability. *Tetrahedron* **2005**, *61*, 2675. (g) He, *J*.; Seela, F. Propynyl groups in duplex DNA: stability of base pairs incorporating 7-substituted 8-aza-7-deazapurines or 5-substituted pyrimidines. *Nucleic Acids Res.* **2002**, *30*, *5*485.

23. Bag, S. S.; Kundu, R. Installation/Modulation of the Emission Response via Click Reaction. *J. Org. Chem.* **2011**, *76*, 3348.
24. (a) Grabowksi, Z. R.; Rotkiewicz, K.; Rettig, W. Structural changes accompanying intramolecular electron transfer: focus on twisted intramolecular charge-transfer states and structures. *Chem. Rev.* **2003**, *103*, 3899. (b) Lakowicz, *J*. R. *Principles of Fluorescence Spectroscopy*, Springer,New York, 3rd edn, **2006**. (c) Yang, S.-W.; Elangovan, A.; Hwang, K.-C.; Ho, T.-I. Electronic Polarization Reversal and Excited State Intramolecular Charge Transfer in Donor/Acceptor Ethynylpyrenes. *J. Phys. Chem.B* **2005**, *109*, 16628. (d) Benniston, A. C.; Harriman, A.; Lawrie, D. *J*.; Mayeux, A. The photophysical properties of a pyrene–thiophene–terpyridine conjugate and of its zinc(II) and ruthenium(II) complexes. *Phys. Chem. Chem. Phys.* **2004**, *6*, 51. (e) Benniston, A. C.; Harriman, A.; Lawrie, D. *J*.; Mayeux, A.; Rafferty, K.; Russell, O. D. A general purpose reporter for cations: absorption, fluorescence and electrochemical sensing of zinc(II). *Dalton Trans.* **2003**, 4762. (f) Strehmel, B.; Seifert, H.; Rettig, W. Photophysical Properties of Fluorescence Probes. 2. A Model of Multiple Fluorescence for Stilbazolium Dyes Studied by Global Analysis and Quantum Chemical Calculations. *J. Phys. Chem. B* **1997**, *101*, 2232. (g) Kim, *J*.; Lee, M. Excited-State Photophysics and Dynamics of a Hemicyanine Dye in AOT Reverse Micelles. *J. Phys. Chem. A* **1999**, *103*, 3378.
25. (a) Badger, G. M.; Walker, I. S. Polynuclear heterocyclic systems. Part IX. n-π*-Transitions in the spectra of aromatic aza-hydrocarbons. *J. Chem. Soc.* **1956**, 122. (b)

Albinsson, B. Dual Fluorescence from N6,N6-Dimethyladenosine. *J. Am. Chem. Soc.* **1997**, *119*, 6369. (c) Chen, X.; Zhao, Y.; Cao, Z. Theoretical study on the dual fluorescence of 2-(4-cyanophenyl)-N,N-dimethylaminoethane and its deactivation pathway. *J. Chem. Phys.* **2009**, *130*, 144307. (d) Thiagara*J*an, V.; Selvaraju, C.; Malar, E. *J*. P.; Ramamurthy, P. A Novel Fluorophore with Dual Fluorescence: Local Excited State and Photoinduced Electron-Transfer-Promoted Charge-Transfer State. *Chem. Phys. Chem.* **2004**, *5*, 1200. (e) Pham, T. H. N.; Clarke, R. *J*. Solvent Dependence of the Photochemistry of the Styrylpyridinium Dye RH421. *J. Phys. Chem. B* **2008**, *112*, 6513. (f) Shim, T.; Lee, M. H.; Kim, D.; Ouchi, Y. Comparison of Photophysical Properties of the Hemicyanine Dyes in Ionic and Nonionic Solvents. *J. Phys. Chem. B.* **2008**, *112*, 1906.(g) Panigrahi, M.; Dash, S.; Patel, S.; Behera, P. K.; Mishra, B. K. Reversal in solvatochromism in some novel styrylpyridinium dyes having a hydrophobic cleft. *Spectrochim. Acta, Part A* **2007**, *68*, 757.

26. (a) Mataga, N.; Kaifu, Y.; Koizumi, M. Solvent Effects upon Fluorescence Spectra and the Dipolemoments of Excited Molecules. *Bull. Chem. Soc. Jpn.* **1956**, *29*, 465. (b) Dahiya, P.; Maity, D. K.; Nayak, S. K.; Mukherjee, T.; Pal, H. Photophysical properties of 1-N-methylamino- and 1-N,N-dimethylamino-9,10-anthraquinone dyes: A comparison with 1-amino-9,10-anthraquinone dye. *J.Photochem. Photobiol. A: Chem.* **2007**, *186*, 218. (c) Masuhara, H.; Mataga, N. Ionic photodissociation of electron donor-acceptor systems in solution. *Acc. Chem. Res.* **1981**, *14*, 312. (d) Lippert, V. Z. Dipolmoment und Elektronenstruktur von angeregten Molekülen. *Z. Naturforsch.* **1955**, *10a*, 541. (e) Dahiya, P.; Kumbhakar, M.; Maity, D. K.; Mukher*J*ee, T.; Tripathi, A. B. R.; Chattopadhyay, N.; Pal, H. Solvent polarity and intramolecular hydrogen bonding effects on the photophysical properties of 1-amino-9,10-anthraquinone dye. *J. Photochem. Photobiol. A: Chem.* **2006**, *181*, 338.

27. (a) Benniston, A. C.; Harriman, A.; LIarena, I.; Sams, C. A. Intramolecular Delayed Fluorescence as a Tool for Imaging Science: Synthesis and Photophysical Properties of a First-Generation Emitter. *Chem. Mater.* **2007**, *19*, 1931. (b) Kim, H. *J.*; Hong, *J.*; Hong, A.; Ham, S.; Lee, *J.* H.; Kim, *J.* S. Cu2+-Induced Intermolecular Static Excimer Formation of Pyrenealkylamine. *Org. Lett.* **2008**, *10*, 1963. (c) Perez-Inestrosa, E.; Montenegro, *J.*-M.; Collado, D.; Suau, R. A molecular 1 : 2 demultiplexer. *Chem. Commun.* **2008**, 1085. (d) Shaikh, M.; Mohanty, *J.*; Singh, P. K.; Bhasikuttan, A. C.; Rajule,R. N.; Satam,V. S.; Bendre, S. R.; Kanetkar, V. R.; Pal, H. Contrasting Solvent Polarity Effect on the Photophysical Properties of Two Newly Synthesized Aminostyryl Dyes in the Lower and in the Higher Solvent Polarity Regions. *J. Phys. Chem. A* **2010**, *114*, 4507. (e) Senthilkumar, S.; Nath, S.; Pal, H. Photophysical properties of coumarin-30 dye in aprotic and protic solvents of varying polarities. *Photochem. Photobiol.* **2004**, *80*, 104. (f) Barik, A.; Nath, S.; Pal, H. Effect of solvent polarity on the photophysical properties of coumarin-1 dye. *J. Chem. Phys.* **2003**, *119*, 10202. (g) Nath, S.; Pal, H.; Sapre, A. V. Effect of solvent polarity on the aggregation of fullerenes: a comparison between C60 and C70. *Chem. Phys. Lett.* **2002**, *360*, 422.

28. Frisch, M. *J.*; Trucks, G. W.; Schlegel, H. B.; Scuseria, G. E.; Robb, M. A.; Cheeseman, *J.* R.; Montgomery, *J.* A., *J*r.; Vreven, T.; Kudin, K. N.; Burant, *J.* C.; Millam, *J.* M.; Iyengar, S. S.; Tomasi, *J.*; Barone, V.; Mennucci, B.; Cossi, M.; Scalmani, G.; Rega, N.; Petersson, G. A.; Nakatsu*J*i, H.; Hada, M.; Ehara, M.; Toyota, K.; Fukuda, R.; Hasegawa, *J.*; Ishida, M.; Naka*J*ima, T.; Honda, Y.; Kitao, O.; Nakai, H.; Klene, M.; Li, X.; Knox, *J.* E.; Hratchian, H. P.; Cross, *J.* B.; Bakken, V.; Adamo, C.; *J*aramillo, *J.*; Gomperts, R.; Stratmann, R. E.; Yazyev, O.; Austin, A. *J.*; Cammi, R.; Pomelli, C.; Ochterski, *J.* W.; Ayala, P. Y.; Morokuma, K.; Voth, G. A.; Salvador, P.; Dannenberg, *J. J.*; Zakrzewski, V. G.; Dapprich, S.; Daniels, A. D.; Strain, M. C.; Farkas, O.; Malick,

D. K.; Rabuck, A. D.; Raghavachari, K.; Foresman, *J*. B.; Ortiz, *J*. V.; Cui, Q.; Baboul, A. G.; Clifford, S.; Cioslowski, *J*.; Stefanov, B. B.; Liu, G.; Liashenko, A.; Piskorz, P.; Komaromi, I.; Martin, R. L.; Fox, D. *J*.; Keith, T.; Al-Laham, M. A.; Peng, C. Y.; Nanayakkara, A.; Challacombe, M.; Gill, P. M. W.; *J*ohnson, B.; Chen, W.; Wong, M. W.; Gonzalez, C.; Pople, *J*. A. *Gaussian 09*, revision C.09; Gaussian, Inc.: Wallingford, CT, **2009**.

29. (a) Bag, S. S.; Jana, S.; Pradhan, M. K. Synthesis, photophysical properties of triazolyl-donor/acceptor chromophores decorated unnatural amino acids: Incorporation of a pair into Leu-enkephalin peptide and application of triazolylperylene amino acid in sensing BSA. *Bioorg. Med. Chem.* **2016**, *24*, 3579 and references therein. (b) Fromherz, P. Monopole-Dipole Model for Symmetrical Solvatochromism of Hemicyanine Dyes. *J. Phys. Chem.***1995**, *99*, 7188. (c) Ji, L.; Lorbach, A.; Edkins, R. M.; Marder, T. B. Synthesis and Photophysics of a 2,7-Disubstituted Donor–Acceptor Pyrene Derivative: An Example of the Application of Sequential Ir-Catalyzed C–H Borylation and Substitution Chemistry. *J. Org. Chem*. **2015**, *80*, 5658. (d) Bucevicius, J.; Skardziute, L.; Dodonova, J.; Kazlauskas, K.; Bagdziunas, G.; Jursenas, S.; Tumkevicius, S. 2,4-Bis(4-aryl-1,2,3-triazol-1-yl)pyrrolo[2,3-d]pyrimidines: synthesis and tuning of optical properties by polar substituents. *RSC Adv.* **2015**, *5*, 38610. (e) Nagarajan, N.; Velmurugan, G.; Venuvanalingam, P.; Renganathan, R. Tunable single and dual emission behavior of imidazole fluorophores based on D-π-A architecture. *J. Photochem. Photobiol. A: Chemistry* **2014**, *284*, 36.

30. Uppuluri, K. B.; Ahmed, K. B. A.; Jothi, A.;Veerappan, A. Spectrofluorimetric and molecular docking investigation on the interaction of 6-azauridine, a pyrimidine nucleoside antimetabolite, with serum protein. *J. Mol. Liq.* **2016**,*219*, 602.

31. Jordheim, L.P.; Durantel, D.;Zoulim, F.; Dumontet, C. Advances in the development of nucleoside and nucleotide analogues for cancer and viral diseases. *Nat. Rev. Drug Discov.* **2013**, *12*, 447.

32. (a) Guallar, V.; Borrelli, K. W. A binding mechanism in protein–nucleotide interactions: Implication for U1A RNA binding. PNAS **2005**, 102, 3954.(b) Wotring, L.L.; Townsend, L.B. Identification of 6-Azauridine Triphosphate in L1210 Cells and Its Possible Relevance to Cytotoxicity. *Cancer Res.***1989**, *49*, 289.

33. Johnson, Z. L.; Lee, J.-H.; Lee, K.; Lee, M.; Kwon, D.-Y.; Hong, J.; Lee, S.-Y. Structural basis of nucleoside and nucleoside drug selectivity by concentrative nucleoside transporters. *eLife* **2014**, *3*, e03604.

34. (a) Vilcheze, C; Jacobs, W.R. Jr. The mechanism of isoniazid killing: clarity through the scope of genetics. *Annu. Rev. Microbiol.* **2007**, *61*, 35.(b) Parker, W.B.; Long, M. C. Purine metabolism in Mycobacterium tuberculosis as a target for drug development. *Curr. Pharm. Des.* **2007**, *13*, 599.

35. Gelamo, E.; Silva, C.; Imasato, H.; Tabak, M. Interaction of bovine (BSA) and human (HSA) serum albumins with ionic surfactants: spectroscopy and modelling. *Biochim. Biophys.Acta Protein Struct. Mol. Enzymol.* **2002**, 1594, 84.

36. Ni, Y.; Su, S.; Kokot, S. Spectrofluorimetric studies on the binding of salicylic acid to bovine serum albumin using warfarin and ibuprofen as site markers with the aid of parallel factor analysis. *Anal. Chim. Acta.* **2006**, *580*, 206.

37. (a) Pal, S.; Saha, C. A review on structure-affinity relationship of dietary flavonoids with serum albumins. *J. Biomol. Struct. Dyn.* **2014**, *32*, 1132. (b) Fasano, M.; Curry, S.; Terreno, E.; Galliano, M.; Fanali, G.; Narciso, P.; Notari, S.; Ascenzi, P. The extraordinary ligand binding properties of human serum albumin. *IUBMB Life* **2005**, *57*, 787.

38. Nakamura, A.; Tsukiji, S. Ratiometric fluorescence imaging of nuclear pH in living cells using Hoechst-tagged fluorescein. *Bioorg. Med. Chem. Lett.* **2017**, *27*, 3127 and references therein.

39. (a) Fan, J. L.; Hu, M. M.; Zhan, P.; Peng, X. J. Energy transfer cassettes based on organic fluorophores: construction and applications in ratiometric sensing. *Chem. Soc. Rev.* **2013**, *42*, 29. (b) Lee, M. H.; Kim, J. S.; Sessler, J. L. Small molecule-based ratiometric fluorescence probes for cations, anions, and biomolecules. *Chem. Soc. Rev.* **2015**, *44*, 4185. (c) Doussineau, T.; Schulz, A.; Lapresta-Fernandez, A.; Moro, A.; Körsten, S.; Trupp, S.; Mohr, G. J. On the Design of Fluorescent Ratiometric Nanosensors. *Chem. – Eur. J.* **2010**, *16*, 10290. (d) Feng, Y.; Cheng, J. H.; Zhou, L.; Zhou, X. G.; Xiang, H. F. Ratiometric optical oxygen sensing: a review in respect of material design. *Analyst* **2012**, *137*, 4885. (e) Demchenko, A. P. The concept of λ-ratiometry in fluorescence sensing and imaging. *J. Fluoresc.* **2010**, *20*, 1099.

40. (a) Deniz, A. A.; Laurence, T. A.; Dahan, M.; Chemla, D. S.; Schultz, P. G.; Weiss, S. Ratiometric single molecule studies of freely diffusing biomolecules. *Annu. Rev. Phys. Chem.* **2001**, *52*, 233. (b) Wu, C.; Zheng, J.; Huang, C.; Lai, J.; Li, S.; Chen, C.; Zhao, Y. Hybrid Silica–Nanocrystal–Organic Dye Superstructures as Post-Encoding Fluorescent Probes. *Angew. Chem. Int. Ed. Engl.* **2007**, *46*, 5393. (c) Wu, P.; Hou, X.; Xu, J.-J.; Chen, H.-Y. Ratiometric fluorescence, electrochemiluminescence, and photoelectrochemical chemo/biosensing based on semiconductor quantum dots. *Nanoscale* **2016**, *8*, 8427.

41. (a) Bikadi, Z.; Hazai, E. Application of the PM6 semi-empirical method to modeling proteins enhances docking accuracy of AutoDock. *J. Cheminf.* **2009**, *1*, 15. (b) Morris, G.M.; Huey, R.; Lindstrom, W.; Sanner, M.F.; Belew, R.K.; Goodsell, D.S.; Olson, A.

J. AutoDock4 and AutoDockTools4: Automated docking with selective receptor flexibility. *J. Comput. Chem.* **2009**, *16*, 2785.

42. Bag, S. S.; Jana, S.; Pradhan, M. K. Synthesis, photophysical properties of triazolyl-donor/acceptor chromophores decorated unnatural amino acids: Incorporation of a pair into Leu-enkephalin peptide and application of triazolylperylene amino acid in sensing BSA. *Bioorg. Med. Chem.* **2016**, *24*, 3579.
43. (a) Monnereau, C.; Blart, E.; Odobel, F. A cheap and efficient method for selective para-iodination of aniline derivatives. *Tetrahedron Lett.* **2011**, *46*, 5421. (b) Tayama, E.; Sugai, S. A facile method for the stereoselective preparation of (1E,3E)-4-substituted-1-amino-1,3-dienes via 1,4-elimination. *Tetrahedron Lett.* **2007**, *48*, 6163.
44. (a) Heinrich, D.; Wagner, T.; Diederichsen, U. Synthesis and DNA Incorporation of an Ethynyl-Bridged Cytosine C-Nucleoside as Guanosine Surrogate. *Org. Lett.* **2007**, *9*, 5311. (b) Semioshkina, A.; Ilinovaa, A.; Lobanovaa, I.; Bregadzea, V.; Paradowskab, E.; Studzinskab, M.; Jabłonskab, A.; Lesnikowskib, Z.J. Synthesis of the first conjugates of 5-ethynyl-2′-deoxyuridine with closo-dodecaborate and cobalt-bis-dicarbollide boron clusters. *Tetrahedron.* **2013**, *69*, 8034. (c) Reddy, M.R.; Shibata, N.; Kondo, Y.; Nakamura, S.; Toru, T. Design, Synthesis, and Spectroscopic Investigation of Zinc Dodecakis(trifluoroethoxy)phthalocyanines Conjugated with Deoxyribonucleosides. *Angew.Chem., Int. Ed.* **2006**, *45*, 8163.
45. (a) Morris, G. M.; Goodsell, D. S.; Halliday, R.S.; Huey, R.;Hart, W.E.; Belew, R.K. Automated docking using a Lamarckian genetic algorithm and an empirical binding free energy function. *J. Comput. Chem.* **1998**, *19*, 1639. (b) Morris, G.M.;Huey, R.;Lindstrom, W.;Sanner, M.F.;Belew, R.K. et al., AutoDock4 and AutoDockTools4: Automated docking with selective receptor flexibility. *J.Comput. Chem.* **2009**, *30*, 2785.

46. (a) Singh, P.; Talwar, P. Exploring putative inhibitors of Death Associated Protein Kinase 1 (DAPK1) via targeting Gly-Glu-Leu (GEL) and Pro-Glu-Asn (PEN) substrate recognition motifs. *J. Mol. Graph. Model.* **2017**, *77*, 153. (b) Vijesh, A.M.; Isloor, A. M.;Telkar, S.;Arulmoli, T.; Fun, H.-K. Molecular docking studies of some new imidazole derivatives for antimicrobial properties. *Arab. J. Chem.* **2013**, *6*, 197. (c) https://projects.biotec.tu-dresden.de/plip-web/plip/index (d) Salentin, S. ; Schreiber, S.; Haupt, V. J.; Adasme, M. F.; Schroeder, M. PLIP: fully automated protein-ligand interaction profiler. *Nucleic Acids Res.* **2015**, *43*, W443.